



Citation for published version:

Fang, C, Nagy-Staron, A, Grafe, M, Heermann, R, Jung, K, Gebhard, S & Mascher, T 2017, 'Insulation and wiring specificity of BceR-like response regulators and their target promoters in *Bacillus subtilis*', *Molecular Microbiology*, vol. 104, no. 1, pp. 16-31. <https://doi.org/10.1111/mmi.13597>

DOI:

[10.1111/mmi.13597](https://doi.org/10.1111/mmi.13597)

Publication date:

2017

Document Version

Peer reviewed version

[Link to publication](#)

This is the peer reviewed version of the following article: Fang, C., Nagy-Staron, A., Grafe, M., Heermann, R., Jung, K., Gebhard, S. and Mascher, T. (2017), Insulation and wiring specificity of BceR-like response regulators and their target promoters in *Bacillus subtilis*. *Molecular Microbiology*, 104: 16–31. doi:10.1111/mmi.13597, which has been published in final form at: <https://doi.org/10.1111/mmi.13597>

This article may be used for non-commercial purposes in accordance with Wiley Terms and Conditions for Self-Archiving.

University of Bath

Alternative formats

If you require this document in an alternative format, please contact:
openaccess@bath.ac.uk

General rights

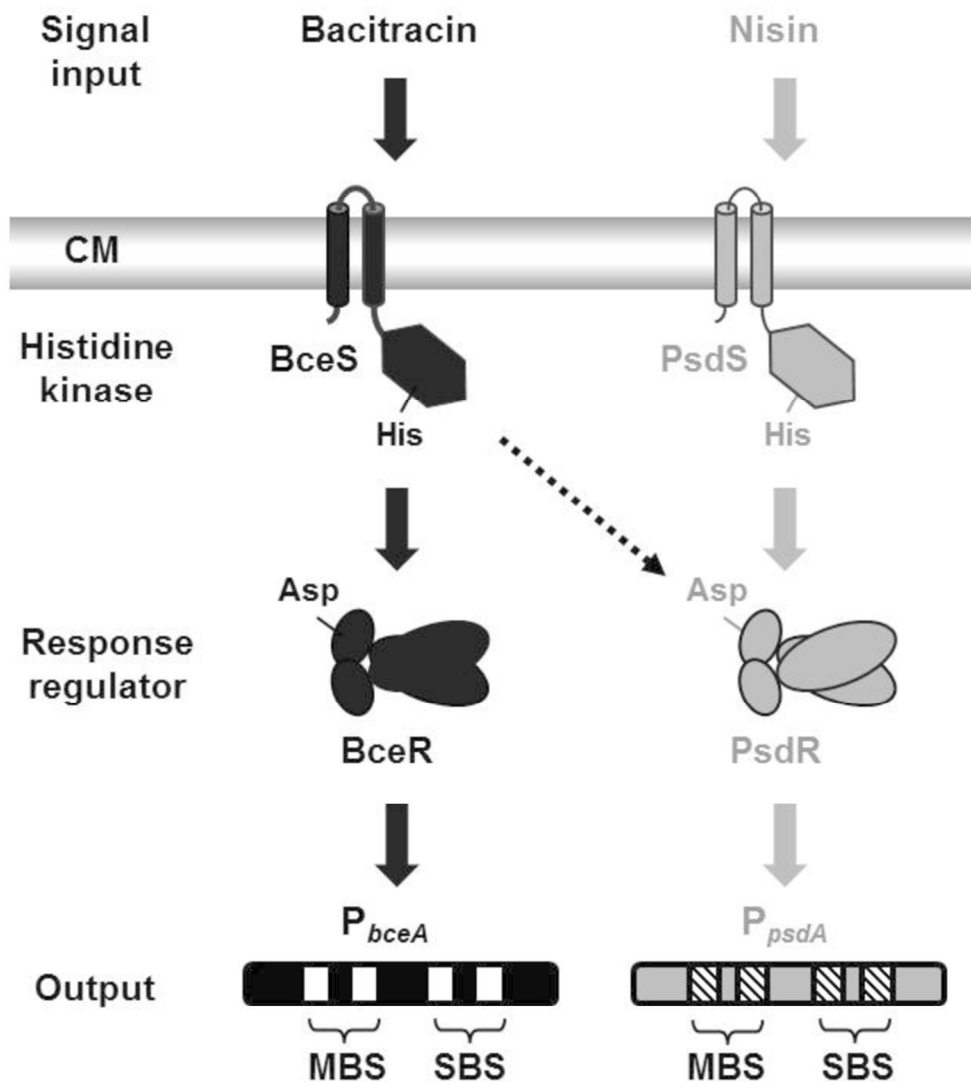
Copyright and moral rights for the publications made accessible in the public portal are retained by the authors and/or other copyright owners and it is a condition of accessing publications that users recognise and abide by the legal requirements associated with these rights.

Take down policy

If you believe that this document breaches copyright please contact us providing details, and we will remove access to the work immediately and investigate your claim.

Insulation and wiring specificity of BceR-like response regulators and their target promoters in *Bacillus subtilis*

Journal:	<i>Molecular Microbiology</i>
Manuscript ID	MMI-2016-16214.R1
Manuscript Type:	Research Article
Date Submitted by the Author:	04-Dec-2016
Complete List of Authors:	Fang, Chong; Ludwig-Maximilians-Universitaet, Biologie/Mikrobiologie Nagy-Staron, Anna; Institute of Science and Technology Austria, n.a. Grafe, Martin; Helmholtz Zentrum Munchen Deutsches Forschungszentrum fur Umwelt und Gesundheit, Research Unit Environmental Genomics Heermann, Ralf; LMU München, Mikrobiologie Jung, Kirsten; Ludwig-Maximilians-Universitaet, Biologie/Mikrobiologie Gebhard, Susanne; University of Bath, Biology and Biochemistry Mascher, Thorsten; Technische Universität Dresden, Institute of Microbiology
Key Words:	two-component system, promoter recognition, antimicrobial peptide resistance, response regulator, DNA-binding site



Model of signal transduction pathways of two Bce-like systems after induction with corresponding AMPs in *Bacillus subtilis*. The TCSs Bce and Psd and their inducing antibiotics as signal inputs are highlighted black and grey, respectively. For reasons of simplicity, the ABC transporters of both systems are not shown. Solid arrows indicate the signal transduction pathway within one system, while cross-regulation between BceS and PsdR is highlighted by the dotted arrow. On each promoter, MBS representing for the main binding site and SBS representing for the secondary binding of Bce-like RRs are filled with white on *bceA* promoter and slashes on *psdA* promoter. CM, cell membrane.

84x94mm (300 x 300 DPI)

Insulation and wiring specificity of BceR-like response regulators and their target promoters in *Bacillus subtilis*

Chong Fang^{1§}, Anna Nagy-Staroń^{1,3§}, Martin Grafe¹, Ralf Heermann^{1,2}, Kirsten Jung^{1,2}, Susanne Gebhard^{1,4}, and Thorsten Mascher^{1,5*}

Abbreviated summary

An efficient insulation is essential to ensure wiring specificity of highly similar signal transducing systems. Here, we describe the regulatory features necessary to allow discrimination of two target promoters by their corresponding paralogous response regulators, involved in mediating resistance against antimicrobial peptides in *Bacillus subtilis*. We demonstrate that regulator competition in combination with hierarchical cooperative binding ensures specificity despite only slight differences in binding affinities.

1

2

3 **Insulation and wiring specificity of BceR-like response regulators and their**
4 **target promoters in *Bacillus subtilis***

5

6 *Chong Fang*^{1§}, *Anna Nagy-Staron*^{1,3§}, *Martin Grafe*¹, *Ralf Heermann*^{1,2}, *Kirsten Jung*^{1,2},
7 *Susanne Gebhard*^{1,4}, and *Thorsten Mascher*^{1,5*}

8

9

10 ¹Department Biology I, Ludwig-Maximilians-Universität München, Großhaderner Str. 2-4, 82152
11 Martinsried, Germany

12 ²Munich Center for Integrated Protein Science (CiPSM) at the Department Biology I, Ludwig-
13 Maximilians-Universität München, Großhaderner Str. 2-4, 82152 Martinsried, Germany

14 ³Institute of Science and Technology (IST) Austria, Am Campus 1, A-3400 Klosterneuburg, Austria

15 ⁴Milner Centre for Evolution, Department of Biology and Biochemistry, University of Bath, Claverton
16 Down, Bath BA2 7AY, United Kingdom

17 ⁵Institute of Microbiology, Technische Universität (TU) Dresden, 01062 Dresden, Germany

18

19 Running title: Wiring specificity of Bce-like systems

20 Key words: two-component system, promoter recognition, antimicrobial peptide resistance, bacitracin,

21 DNA-binding site

22

23 § These two authors contributed equally to this work.

24

25 *To whom correspondence should be addressed. E-mail: thorsten.mascher@tu-dresden.de; Phone: +49
26 351 463-40420

27 **Summary**

28 BceRS and PsdRS are paralogous two-component systems in *Bacillus subtilis* controlling the
29 response to antimicrobial peptides. In the presence of extracellular bacitracin and nisin,
30 respectively, the two response regulators (RRs) bind their target promoters, P_{bceA} or P_{psdA} ,
31 resulting in a strong up-regulation of target gene expression and ultimately antibiotic
32 resistance. Despite high sequence similarity between the RRs BceR and PsdR and their
33 known binding sites, no cross-regulation has been observed between them. We therefore
34 investigated the specificity determinants of P_{bceA} and P_{psdA} that ensure the insulation of these
35 two paralogous pathways at the RR-promoter interface. *In vivo* and *in vitro* analyses
36 demonstrate that the regulatory regions within these two promoters contain three important
37 elements: in addition to the known (main) binding site, we identified a linker region and a
38 secondary binding site that are crucial for functionality. Initial binding to the high affinity,
39 low specificity main binding site is a prerequisite for the subsequent highly specific binding
40 of a second RR dimer to the low affinity secondary binding site. In addition to this
41 hierarchical cooperative binding, discrimination requires a competition of the two RRs for
42 their respective binding site mediated by only slight differences in binding affinities.

43 Introduction

44 Antimicrobial peptides (AMPs) are predominantly produced by Gram-positive microbes to
45 suppress the growth of competitors in their natural habitats (Berdy, 2005). The main target of
46 AMPs is the bacterial cell envelope, especially different intermediates of the lipid II cycle. By
47 binding to their target molecules, AMPs inhibit cell wall biosynthesis and cause cell death
48 (Silver, 2003, Breukink & de Kruijff, 2006, Jordan *et al.*, 2008).

49 In Firmicutes bacteria, sensing of and resistance against AMPs is usually mediated by highly
50 conserved Bce-like detoxification modules containing an ATP-binding-cassette (ABC)
51 transporter and a two-component system (TCS) (Dintner *et al.*, 2011). The genome of
52 *Bacillus subtilis* encodes three such systems: BceRS-BceAB, PsdRS-PsdAB and the poorly
53 understood YxdJK-YxdLM-YxeA system (Joseph *et al.*, 2002, Gebhard & Mascher, 2011).
54 The BceRS-BceAB paradigm responds to AMPs such as bacitracin, actagardine and
55 mersacidin (Staroń *et al.*, 2011, Dintner *et al.*, 2014, Fritz *et al.*, 2015). It consists of two
56 separate operons: the *bceRS* operon encodes the TCS comprised of a membrane anchored
57 histidine kinase (HK), BceS, and a cytoplasmic response regulator (RR), BceR, under the
58 control of a constitutive promoter. The *bceAB* operon encodes the ABC transporter under the
59 control of an inducible BceR-dependent promoter, P_{bceA} . In the absence of AMPs, both
60 operons are expressed at a very low level. In the presence of AMPs such as bacitracin, the
61 ABC transporter BceAB senses this stimulus and passes the signal on to the HK BceS
62 (Dintner *et al.*, 2014). Upon autophosphorylation, BceS then activates its cognate RR BceR
63 by phosphoryl-group transfer. Phosphorylated BceR will then bind to P_{bceA} and strongly
64 induce *bceAB* transcription, ultimately resulting in increased BceAB production, thereby
65 conferring AMP resistance (Mascher *et al.*, 2003, Ohki *et al.*, 2003, Bernard *et al.*, 2007,
66 Rietkötter *et al.*, 2008, Fritz *et al.*, 2015) (Fig. 1 black system, BceAB not shown).

67 The main inducers of the Psd system are lipid II-binding lantibiotics such as nisin, actagardine,
68 gallidermin and subtilin. In turn, the Psd system confers resistance against nisin, actagardine

69 and subtilin (Staroń *et al.*, 2011). The signal transduction pathway within Psd system (Fig. 1
70 grey system, PsdAB not shown) is similar to that described for the Bce system (Gebhard &
71 Mascher, 2011). Despite significant sequence similarity between BceRS-BceAB and PsdRS-
72 PsdAB, signaling in each system is generally well insulated from the other, although a
73 previous study has demonstrated some degree of cross-phosphorylation between BceS and
74 PsdR at high bacitracin concentrations (Rietkötter *et al.*, 2008) (Fig. 1, dotted arrow).

75 In bacteria, transcription initiation starts with promoter recognition by the σ subunit of the
76 RNA polymerase holo-enzyme at the -35 promoter element, followed by binding and
77 unwinding of the DNA double helix at the -10 promoter element (Lee *et al.*, 2012). A -10
78 promoter element with a perfect match to the σ^A consensus sequence (TATAAT) could be
79 identified in P_{bceA} . It is located 6 bp upstream of the transcription initiation site, which is 32 bp
80 upstream of the *bceA* start codon. However, a conserved -35 element was not found (Ohki *et*
81 *al.*, 2003). An identical σ^A -dependent -10 element was also found in P_{psdA} , again lacking a
82 clear -35 element at the appropriate position (Staroń *et al.*, 2011) (Fig. 2A). For such
83 promoters deviating significantly from the consensus sequence at the -35 position, the σ
84 subunit of RNA polymerase can still be recruited to these promoters by interaction with
85 activators like RRs binding to the upstream region (Jarmer *et al.*, 2001, Paget & Helmann,
86 2003). RRs usually contain an N-terminal receiver domain and a C-terminal output domain.
87 Both BceR and PsdR belong to the OmpR/PhoB subfamily of RRs with a C-terminal winged
88 helix-turn-helix DNA-binding output domain that regulates the transcription of target genes
89 by binding to their corresponding promoter regions via a specific recognition motif (Martínez-
90 Hackert & Stock, 1997, Fabret *et al.*, 1999, Galperin, 2010). Inverted repeats on P_{bceA} as well
91 as on P_{psdA} were mapped as BceR- and PsdR-binding sites, respectively, upstream of the
92 corresponding -10 promoter elements (Fig. 2A), which implies an interaction between BceR-
93 like RRs and the RNA polymerase holo-enzyme (Ohki *et al.*, 2003, de Been *et al.*, 2008,
94 Staroń *et al.*, 2011).

95 The DNA binding domains of BceR and PsdR share 51% sequence identity (66% similarity)
96 and the corresponding binding sites on P_{bceA} and P_{psdA} contain eleven out of fourteen identical
97 nucleotides (Fig. 2A) (Joseph *et al.*, 2002). Nevertheless, no cross-regulation was detected at
98 the transcriptional level between BceR- P_{psdA} and PsdR- P_{bceA} (Rietkötter *et al.*, 2008). Such a
99 regulatory insulation, that is, prevention of nonspecific regulatory cross-talk, is of course
100 desired and can arise at different molecular levels *in vivo* (Huynh & Stewart, 2011). The most
101 prominent mechanism for conferring such signaling specificity depends on the molecular
102 recognition between the two interaction partners (Podgornaia & Laub, 2013). However, in the
103 case of the Psd and Bce systems, the high degree of identity between the two regulator
104 binding sites raised the question how specificity can be ensured between two such closely
105 related systems.

106 Here we provide detailed insights into the molecular mechanisms that ensure insulation and
107 transcriptional regulation specificity between two Bce-like systems in *B. subtilis*, Bce and Psd
108 at the level of RR-promoter interaction. Using both *in vivo* and *in vitro* approaches, we
109 identified a secondary RR-binding site in both P_{bceA} and P_{psdA} , in addition to the previously
110 identified (main) binding site. Importantly, we demonstrate that the main binding site, while
111 being essential for promoter activation, does not significantly contribute to specificity of RR-
112 promoter interactions. Instead, the secondary binding site and the variable linker region
113 between the two sites are the primary specificity determinants. Moreover, our data show that
114 *in vivo* promoter discrimination is based on competition between the two RRs for their
115 respective binding sites.

116

117

118 Results

119

120 *Identification of the minimal bceA and psdA promoter motif*

121 P_{bceA} and P_{psdA} are the target promoters for the RRs BceR and PsdR, respectively (Staroń *et al.*, 2011). When *B. subtilis* is challenged with bacitracin, BceR is activated by the
122 corresponding HK BceS and binds to a specific region of P_{bceA} , resulting in a strong
123 upregulation of the operon encoding the ABC transporter for resistance (Mascher *et al.*, 2003)
124 (Fig. 1). Previous work has already mapped an inverted repeat sequence for BceR binding in
125 the P_{bceA} region (AAGCGTGTGACgaaaatGTCACAtGCTT) from -111 to -84 upstream of the
126 *bceA* start codon (Ohki *et al.*, 2003). For P_{psdA} , a highly similar PsdR binding site
127 (ATgTgACAgcatTGTAaAgAT) could be identified from -99 to -80 upstream of the *psdA* start
128 codon (Staroń *et al.*, 2011). In agreement with these studies, a comparative genomics study
129 identified a putative binding site among most *bceA*-like promoters in Firmicutes bacteria, with
130 an overall consensus sequence of TnACA-N₄-TGTAAs as a recognition site for BceR-like RRs
131 (Dintner *et al.*, 2011).
132

133 We first wanted to verify that these two known conserved binding motifs are indeed
134 indispensable for the RR-dependent activation of the *bceA* and *psdA* promoters and identify
135 the minimal regulatory elements for both promoter regions. Towards that goal, progressively
136 truncated *bceA* promoters starting with the 5'-position ranging from -111 to -103 and ending
137 at +82 relative to the ATG start codon of *bceA* were used to construct transcriptional *lacZ*
138 reporter fusions (Table S2), which were integrated at the *amyE* locus in *B. subtilis* 168 wild
139 type (WT) (Table S1). Progressively truncated *psdA* promoter fragments starting with 5'-
140 positions ranging from -110 to -95, all ending at position +30 relative to the ATG start codon
141 of *psdA*, were generated in a similar fashion (Fig. 2A). The promoter activity of the resulting
142 reporter strains was determined by quantitative β -galactosidase assay in the presence of
143 bacitracin (P_{bceA}) or nisin (P_{psdA}) (Staroń *et al.*, 2011).

144 Truncated *bceA* promoters from -111 until -106 showed activities comparable to the non-
145 truncated promoter fragment starting at position -122 after bacitracin induction (black bars)
146 (Fig. 2B). The truncations starting at position -105 and position -104 displayed a decreased
147 promoter activity, while a further truncation of one additional nucleotide (starting at position -
148 103) led to a complete loss of promoter activity after bacitracin induction.

149 Similar results were obtained for truncated *psdA* promoter fragments after nisin induction
150 (grey bars) (Fig. 2C). No decrease of promoter activity was observed for truncations with 5'-
151 positions starting from -110 to -100 relative to the positive control fragment, starting at
152 position -126. The promoter activities were significantly reduced for fragments truncated at
153 positions -99 to -96, while a truncation at position -95 led to a complete loss of activity after
154 nisin induction.

155 These data confirmed that the 7-4-7 nt binding motif TGTGACGaaaTGTCACA of P_{bceA} and
156 the TGTGACAgcatTGTAAGA binding motif of P_{psdA} are indeed necessary for promoter
157 induction and constitute likely binding sites for BceR and PsdR, in good agreement with
158 previous reports (Ohki *et al.*, 2003, de Been *et al.*, 2008, Staroń *et al.*, 2011). These will be
159 referred to as “main binding sites” (MBSs) from now on. Position -104 relative to *bceA* start
160 codon and position -96 relative to *psdA* start codon determine the minimal 5'-end of active
161 RR-dependent promoter fragments.

162

163 ***A secondary binding site on bceA and psdA promoters***

164 Sequence analysis of P_{bceA} and P_{psdA} did not identify a typical -35 region (TTGACA) upstream
165 of the -10 region as normally recognized by σ^A (Jarmer *et al.*, 2001). However, a 7 nt
166 conserved half binding site for a BceR-like RR, located 13/14 nt downstream of the MBS and
167 38 nt upstream of the -10 region, was predicted for both the *bceA* and the *psdA* promoter
168 regions (Dintner *et al.*, 2011). This observation implies the existence of a secondary binding
169 site (SBS) instead of a typical -35 element on *bceA*-like promoters. Based on this prediction,

170 we annotated a putative SBS also showing the 7-4-7 pattern, as well as a linker region (L)
171 between the MBS and the SBSs on both *bceA* and *psdA* promoters (Fig. 2A). We
172 experimentally investigated the function of the predicted promoter motifs by randomizing
173 their sequence, while maintaining the GC/AT content of the linker region. The fragments
174 were used to generate *lacZ* reporter gene fusions (Tables 1+2) and were assayed as before.

175 Both the WT *bceA* promoter (Fig. 2D) and the *psdA* promoter (Fig. 2E) showed strong
176 induction with the corresponding inducers bacitracin (black bars) or nisin (grey bars)
177 compared to the non-induced samples (white bars), but no such response to the non-cognate
178 inducer. The weak induction of P_{psdA} by bacitracin (Fig. 2E) was due to the known cross-
179 phosphorylation of PsdR by BceS (Rietkötter *et al.*, 2008) (Fig. 1 dotted arrow). Randomizing
180 the MBS led to a complete loss of activity for both promoters. The same effect was obtained
181 when randomizing the sequence of the predicted SBS. However, activities of both *bceA* and
182 *psdA* promoters only showed a slight decrease by randomly mutating the corresponding linker
183 region (L) between the two binding sites (Fig. 2D and 2E).

184 The data demonstrate that on both P_{bceA} and P_{psdA} , a SBS exists that is located downstream of
185 the MBS with a 13/14 nt linker region in between them. This SBS seemingly replaces the -35
186 region and is as indispensable as the MBS for RR-dependent promoter activity. Additional
187 assays done by randomizing either the first or the second half of each SBS were in agreement
188 with the results obtained for the completely randomized SBSs (data not shown), further
189 demonstrating that each half binding site has the same importance for P_{bceA} and P_{psdA} activity.

190

191 ***Major specificity determinants are located in the region containing linker and SBS***

192 So far, we have identified an extended regulatory region in P_{bceA} and P_{psdA} , consisting of two
193 binding sites, MBS and SBS, and a linker region between them. Since there is no cross-
194 regulation at the RR-promoter interface, neither between BceR- P_{psdA} nor PsdR- P_{bceA}
195 (Rietkötter *et al.*, 2008), we therefore wanted to analyse the specificity determinants within

196 the *bceA/psdA* promoters. Towards that goal, a series of chimeric promoters derived from
197 P_{bceA} and P_{psdA} was constructed (Table S2) and fused with *lacZ*. Chimeric promoters BP1-4
198 are derived from P_{bceA} (black) with gradually substituting P_{psdA} (grey) at the 3'-terminal end
199 (Fig. 3A). Chimeric promoters PB1-4 are derived from P_{psdA} (grey) with increasing of 3'-
200 fragments from P_{bceA} (black) (Fig. 3B). To specifically eliminate any cross-talk between the
201 Bce and Psd systems, the chimeric promoters as well as WT P_{bceA} and WT P_{psdA} fragments as
202 references, were introduced into the WT strain and additionally the otherwise isogenic
203 $\Delta bceRS$ (TMB1460) and the $\Delta psdRS$ (TMB1462) strains (Table S1). Compared to the WT
204 strain, the $\Delta bceRS$ and $\Delta psdRS$ backgrounds remove the effect of cross-phosphorylation and
205 hence provide a clearer view of individual RR-promoter interactions.

206 P_{bceA} showed the same high activity in the $\Delta psdRS$ mutant (Fig. 3D) as in the WT strain (Fig.
207 3C) after bacitracin induction, but no activity after nisin induction in either the WT (Fig. 3C)
208 or the $\Delta bceRS$ background (Fig. 3E). Correspondingly, P_{psdA} was highly induced by nisin in
209 both the WT strain (Fig. 3C) and the $\Delta bceRS$ mutant (Fig. 3E). Importantly, the moderate
210 induction of P_{psdA} by bacitracin seen in the WT (Fig. 3C) was not detected in the $\Delta bceRS$
211 mutant (Fig. 3D) due to the elimination of cross-phosphorylation between BceS and PsdR.
212 These results are in agreement with previous studies that there is no cross-regulation at the
213 RR-promoter level.

214 Chimeric promoters BP1 and BP2 showed high activity after induction with bacitracin in both
215 the WT strain (Fig. 3C) and the $\Delta psdRS$ strain (Fig. 3D), but no activity upon nisin induction
216 in either the WT strain (Fig. 3C) or the $\Delta bceRS$ strain (Fig. 3E). Hence, BP2 could be
217 recognized by BceR, but not by PsdR. These results indicate that the specificity determinants
218 are located within the region upstream of and including the SBS. Interestingly, the chimeric
219 promoter BP3 could neither be induced by bacitracin in the $\Delta psdRS$ background (Fig. 3D) nor
220 by nisin in the $\Delta bceRS$ background (Fig. 3E), but showed moderate induction by bacitracin in
221 only the WT background (Fig. 3C). The observation that PB3 requires both TCSs for

222 responding to bacitracin might point towards the formation of RR heterodimers. But this
223 interpretation is purely speculative at the moment and will require follow-on studies.
224 Moreover, BP4 – possessing the whole region downstream of the MBS originating from P_{psdA}
225 – was not only moderately induced by bacitracin in the $\Delta psdRS$ background (Fig. 3D) but also
226 by nisin in the $\Delta bceRS$ background (Fig. 3E), indicating a relaxation of specificity from BceR
227 to PsdR. The results of BP2 and BP4 demonstrate that the major specificity determinants of
228 P_{psdA} are located in the region containing the linker and the SBS.

229 Chimeric promoters PB1 and PB2 showed a decreased activity after induction with nisin in
230 both the WT background (Fig. 3F) and the $\Delta bceRS$ mutant (Fig. 3G) relative to P_{psdA} , and no
231 bacitracin induction in the $\Delta psdRS$ mutant (Fig. 3H), indicating no change of specificity.
232 These results corroborate that the region downstream of the SBS is not relevant for the RR-
233 promoter specificity. Interestingly, PB3 showed a significantly decreased activity in the
234 $\Delta bceRS$ mutant with nisin induction (Fig. 3G) and a strongly increased activity in the $\Delta psdRS$
235 mutant with bacitracin induction (Fig. 3H). Chimera PB4 was not inducible by nisin in the
236 $\Delta bceRS$ strain (Fig. 3G), but instead showed high induction by bacitracin in the $\Delta psdRS$ strain
237 (Fig. 3H), strongly reminiscent of the intact P_{bceA} . The promoter activities of PB3 and PB4 in
238 the WT strain (Fig. 3F) were in accordance with those observed in both mutant backgrounds.
239 These data indicate that the change of specificity from P_{psdA} to P_{bceA} can be achieved by
240 exchanging the SBS (PB3), and is further strengthened by an additional substitution of the
241 linker region (PB4).

242 The analysis of chimeric promoter constructs described above demonstrates that (i) all three
243 regulatory parts (MBS-linker-SBS) together determine the RR-specificity, with (ii) the region
244 downstream of the MBS of P_{bceA}/P_{psdA} , containing the linker and the SBS, functioning as the
245 main discriminator for BceR/PsdR recognition.

246

247 ***Rewiring the specificity between P_{bceA} and P_{psdA} enables dissecting the roles of individual***
248 ***specificity determinants***

249 To further investigate the functions of MBS, linker region and SBS on the *psdA* promoter for
250 PsdR recognition, additional chimeric promoters were generated with different combinations
251 of these three motifs on P_{bceA} replaced by the corresponding region of P_{psdA} (Fig. 4A) to rewire
252 specificity from BceR to PsdR. Promoter activities were measured as described above in the
253 WT strain (Fig. 4C), the $\Delta psdRS$ strain (Fig. 4D) and the $\Delta bceRS$ strain (Fig. 4E).

254 Compared to P_{bceA} , replacing only the MBS (M), the linker (L) or both (M+L) of P_{bceA} with
255 the corresponding region of P_{psdA} showed decreased promoter activity in the WT strain after
256 induction with bacitracin (Fig. 4C) as well as in the $\Delta psdRS$ mutant (Fig. 4D). No increase of
257 the promoter activity after induction by nisin was observed in either the WT strain (Fig. 4C)
258 or the $\Delta bceRS$ mutant (Fig. 4E). This indicates that the MBS, the linker or both of P_{psdA} are
259 not enough to cause activation via PsdR. Changing the SBS (S) on P_{bceA} into P_{psdA} led to a
260 decrease of promoter activity after induction with bacitracin in the WT strain (Fig. 4C) as well
261 as in the $\Delta psdRS$ mutant (Fig. 4D) and a slight but detectable increase of promoter activity
262 after induction with nisin in the $\Delta bceRS$ mutant (Fig. 4E). This indicates that exchanging only
263 the SBS alone already conferred a relaxation of promoter specificity from BceR to PsdR.

264 Substitution of the linker together with the SBS (L+S) resulted in a higher promoter activity
265 compared to only exchanging the SBS (S) both after bacitracin induction (Fig. 4D) and nisin
266 induction (Fig. 4E). This indicates that the linker region (L) can enhance promoter activity
267 with both cognate PsdR and noncognate BceR. Compared to only the SBS switch (S),
268 exchanging both the MBS and the SBS simultaneously (M+S) resulted in a severe decrease of
269 the promoter activity after induction with bacitracin (Fig. 4D), while causing an increase of
270 the promoter activity after induction with nisin (Fig. 4E).

271 Taken together, these results suggest that the SBS on P_{psdA} is the main discriminator for PsdR-
272 binding to P_{psdA} , even though the intensity of induction with the SBS substitution alone is not

273 very strong. The linker cannot determine specificity by itself but can increase promoter
274 activity with both BceR and PsdR, which explains the change of specificity that was detected
275 for construct BP4 including the linker and the SBS but not for construct BP3 with only the
276 SBS (Fig. 3C). Despite the fact that the MBS is absolutely crucial for RR-promoter
277 interaction, the MBS of P_{psdA} alone cannot determine specificity. Instead, it supports the SBS
278 in strengthening the promoter activity. Not surprisingly, switching all three elements together
279 (M+L+S) resulted in the highest change of specificity after induction with nisin (Fig. 4E),
280 demonstrating that all three parts together contribute to the specificity.

281 In order to support the results obtained above, a similar approach was performed towards
282 rewiring the specificity from P_{psdA} to P_{bceA} . A comparable series of chimeric promoters with
283 different combinations of the MBS, the linker region and the SBS of P_{psdA} being replaced by
284 the corresponding regions from P_{bceA} was constructed (Fig. 4B) (Table S2) and the promoter
285 activities of the corresponding *B. subtilis* reporter strains (Table S1) were determined. The
286 results are shown in Fig. 4F-4H. Overall, the combined data is in very good agreement with
287 the results obtained for rewiring the specificity from P_{psdA} to P_{bceA} with only minor differences
288 between the two sets.

289 Taken together, exchanging the MBS alone had no effect on the specificity of induction of
290 P_{bceA} and only caused a very minor change in P_{psdA} behaviour. Instead, the SBS provides the
291 major discriminator for RR binding. The data is particularly clear for the BceR- P_{bceA}
292 interaction, where exchange of the SBS alone was able to cause a clear change in specificity,
293 while the role of the SBS of P_{psdA} for the PsdR- P_{psdA} pair is less prominent. Both promoters
294 have in common that the MBSs strengthen the specificity by increasing the interactions with
295 the cognate RR, while simultaneously reducing the interactions with the non-cognate RR. In
296 addition, the linker regions fine tune promoter activity. While specific roles can therefore be
297 attributed to these three regulatory elements, it should be pointed out that the specificity of

298 BceR-like RRs for their target promoters is ultimately determined by the specific combination
299 of MBS, linker and SBS working together.

300

301 **In vitro analysis of BceR binding to P_{bceA} and P_{psdA}**

302 Next, we wanted to investigate if BceR could also discriminate between its native promoter
303 P_{bceA} and the non-cognate P_{psdA} *in vitro*. BceR carrying an N-terminal His₁₀-tag with the
304 expected molecular mass of about 27 kDa was produced in and purified from the cytoplasmic
305 fraction of *E. coli* C43(DE3) cells containing plasmid pCF120 (Table S2). Electrophoretic
306 mobility shift assays (EMSAs) were performed with purified BceR and the two promoters
307 P_{bceA} and P_{psdA} . 300 bp promoter DNA fragments (300 bp) of P_{bceA} or P_{psdA} containing the
308 MBS, the linker region and the SBS were amplified and labeled at the 5'-end with 6FAM by
309 PCR. 6FAM labeled P_{sigW} (the target promoter of an ECF sigma factor in *B. subtilis*) was used
310 as a negative control.

311 The results of EMSAs with BceR and P_{bceA} are shown in Figure 5A. Increasing concentrations
312 of BceR phosphorylated by the addition of phosphoramidate (BceR-P; see Experimental
313 procedure) were incubated with 30 fmol of 6FAM- P_{bceA} (lane 2 to lane 5), demonstrating a
314 concentration-dependent binding of BceR-P to P_{bceA} . The first shift was observed at 1.0 μ M
315 BceR-P representing the initial binding event of BceR-P to P_{bceA} . An additional shift occurred
316 at BceR-P concentrations of 1.5 μ M or above and presumably represents a second binding
317 event, consistent with the presence of two BceR binding sites on the DNA fragment. In
318 contrast, unphosphorylated BceR showed a much weaker binding (data not shown), which
319 demonstrated that RR-phosphorylation promotes DNA binding by increasing BceR affinity to
320 P_{bceA} .

321 EMSAs were also performed between BceR-P and P_{psdA} (Fig. 5B). Two successive shifts of
322 P_{psdA} band in lane 3 and lane 4 compared to free P_{psdA} DNA fragment (lane 1) demonstrated
323 that BceR-P can also bind to two sites in the noncognate but highly related P_{psdA} *in vitro*. In

324 contrast, no shift was observed for the P_{sigW} DNA fragment (Fig. 5E), confirming the overall
325 specificity of the assay: BceR-P cannot bind to promoter fragments that do not harbor the
326 binding motifs of a P_{bceA} -like promoter.

327 To further illustrate the specificity and affinities of BceR-P binding to P_{bceA} and P_{psdA} , 900
328 fmol of unlabeled promoter fragments were used as competitor DNA (Fig. 5A/5B lane 6-8).
329 Co-incubation of BceR-P with 30 fmol 6FAM- P_{bceA} and 900 fmol unlabeled P_{bceA} fragment
330 (Fig. 5A lane 6) completely abolished the retardation of the labeled P_{bceA} fragment due to the
331 competitive binding of BceR-P to an excess of unlabeled P_{bceA} . However, the shift of 6FAM-
332 P_{bceA} band was not influenced by adding a 30-fold molar excess of unlabeled P_{psdA} (Fig. 5A
333 lane 7) or P_{sigW} (Fig. 5A lane 8). This shows that despite its ability to bind to both P_{bceA} and
334 P_{psdA} in isolation, BceR is clearly able to distinguish between the two promoters and
335 preferentially binds to its cognate target. In contrast, the retardation of the 6FAM- P_{psdA} DNA
336 fragment was abolished by either addition of 30-fold excess unlabeled P_{bceA} (Fig. 5B lane 6)
337 or unlabeled P_{psdA} (Fig. 5B lane 7) fragments but not by P_{sigW} (Fig. 5B lane 8). These results
338 clearly demonstrate that, while BceR-P can interact with seemingly identical activities with
339 both target promoters in isolation (the shift occurs at comparable BceR-P concentrations), it
340 preferentially binds to its native promoter, P_{bceA} , compared to P_{psdA} *in vitro* when incubated in
341 competition. Hence, the binding affinity for its cognate target promoter P_{bceA} seems to be
342 higher than for P_{psdA} , which determines the *in vivo* specific transcription initiation.
343 Unfortunately, any efforts to purify PsdR failed, thereby preventing the performance of
344 similar *in vitro* studies on PsdR- P_{psdA} / P_{bceA} interactions.

345

346 ***Cooperative binding of BceR to two binding sites on P_{bceA}***

347 The *in vivo* promoter activity assays demonstrated that both binding sites on P_{bceA} are
348 indispensable for BceR- P_{bceA} interaction (Fig. 2D). Moreover, the EMSA studies on complete
349 promoter fragments strongly suggest two binding events at P_{bceA} *in vitro* (Fig. 5A). To

350 discriminate between the individual binding reactions, we next performed EMSAs with BceR-
351 P on 6FAM labeled *bceA* promoter DNA-fragments carrying randomized versions of either
352 the MBS or the SBS (Fig. 5D).

353 Incubation of BceR-P with labeled P_{bceA} SBS^R (P_{bceA} containing a native MBS and a
354 randomized and hence inactive SBS) caused only a single shift at a BceR-P concentration of
355 1.0 μ M (Fig. 5C), a concentration comparable to the threshold concentration for binding to
356 the intact P_{bceA} fragment (Fig. 5A lane 3). Increasing the BceR-P concentration did not lead to
357 any additional shift. Hence, P_{bceA} containing only the MBS merely allows one binding event,
358 which is the binding of BceR-P to the MBS. The identical BceR-P concentrations required for
359 shifting either the WT or the SBS^R fragments indicates that binding of BceR-P to the MBS is
360 independent of the SBS.

361 Incubation of BceR-P with labeled P_{bceA} MBS^R (P_{bceA} containing a randomized and hence
362 inactive MBS but an intact SBS) failed to retard the DNA-fragment within the same
363 concentration range (Fig. 5D). This suggests that either BceR-P has a very low affinity for
364 binding to the SBS alone or that binding to the SBS depends on and occurs after BceR-P
365 binding to the MBS.

366

367 ***Determination of binding kinetics of BceR-promoter interaction unravels the mechanism***
368 ***that determines BceR promoter specificity***

369 For quantitatively describing the binding kinetics of BceR-promoter interactions, we next
370 performed SPR spectroscopy in combination with Interaction Map® (IM) analysis. We
371 captured a biotin-labeled DNA-fragment comprising the P_{bceA} region (see Table S3 for exact
372 sequence) to a sensor chip coated with immobilized streptavidin. Next, increasing
373 concentrations of His₁₀-BceR and His₁₀-BceR-P were injected over the chip surface. While
374 non-phosphorylated BceR did not interact with the P_{bceA} promoter (Fig. 6A), BceR-P showed
375 clear binding (Fig. 6B). Since BceR has two binding sites on the DNA-fragment used for SPR,

376 we performed IM analyses. In order to determine and quantify the individual binding events
377 represented by the SPR curves. Briefly, the IM algorithm splits the experimental SPR data set
378 into several theoretical monovalent binding events and selects the binding curves that best fit
379 the experimental data when summed up. By plotting the association rate k_a and the
380 dissociation rate k_d within a two-dimensional distribution, heterogeneous binding data can be
381 displayed as a map, in which each peak corresponds to one component that contributes to the
382 cumulative binding curve (Altschuh *et al.* 2012). The sensorgram could be split into two
383 binding events, one characterized by a fast ON/fast OFF ($k_a=1.8 \times 10^6/\text{M}\cdot\text{s}$; $k_d=1.0 \times 10^{-1}/\text{s}$)
384 and one characterized by a slow ON/slow OFF binding kinetics ($k_a=3.2 \times 10^5/\text{M}\cdot\text{s}$;
385 $k_d=5.5 \times 10^{-4}/\text{s}$) that differ in their overall affinity ($K_D=58 \text{ nM}$ and $K_D=1.7 \text{ nM}$, respectively)
386 (Fig. 6E). Each binding peak makes up an approximate peak weight of 50% revealing that
387 both DNA-binding sites are bound by equal amounts of BceR-P molecules.

388 As a next step, we determined the binding kinetics between BceR-P and P_{bceA} when the MBS
389 or the SBS was randomized (MBS^R or SBS^R, respectively). Inactivation of the MBS
390 completely prevented DNA-binding of BceR-P (Fig. 6C), while a clear DNA-binding of BceR
391 could still be observed when only the SBS was randomized (Fig. 6D). In contrast to the
392 sensorgram including both intact binding sites (Fig. 6B), the IM of the corresponding
393 sensorgram suggested in principle only the slow ON/slow OFF binding event ($k_a=1.5 \times 10^6$
394 $\text{M}\cdot\text{s}$; $k_d=4.9 \times 10^{-4}/\text{s}$, resulting in an overall binding affinity of $K_D=0.4 \text{ nM}$ (Fig. 6F).
395 However, the *in silico* sensorgram is comparable to that one of the slow ON/slow OFF
396 interaction of BceR-P to intact P_{bceA} site revealing that this reflects binding of BceR-P to the
397 MBS although the overall affinity is approximately six-fold higher, mainly caused by the five-
398 fold higher ON rate. The peak weight is calculated as 80%, meaning that this interaction
399 mainly contributes to the measured sensorgram. However, the fast ON/fast OFF peak did not
400 completely disappear, but compared to the intact promoter site the peak weight is lower than
401 20% and can therefore be neglected. These data clearly show that the MBS of the P_{bceA} region

402 is essential for binding of the RR to the DNA. Moreover, the affinity of the RR is not
403 sufficient to allow any binding of BceR to the SBS if the MBS was not previously occupied,
404 at least under the experimental regime applicable for SPR spectroscopy. Comparing the
405 binding kinetics of BceR-P to the intact and the SBS^R promoter, it can be assumed that the
406 SBS increases the overall affinity of the RR to the promoter region, and therefore is important
407 for triggering gene expression.

408 Finally, we wondered if the binding mechanism of BceR-P is also similar to the related P_{psdA}.
409 We captured DNA comprising the P_{psdA} promoter as well as the P_{psdA} promoter in which the
410 MBS or SBS were inactivated (MBS^R or SBS^R, respectively) onto the chip. First, we injected
411 increasing concentrations of non-phosphorylated BceR over the chip and observed, as
412 expected, no binding to the P_{psdA} promoter (Fig. 6G). Then, increasing concentrations of
413 BceR-P were injected. The interaction of BceR-P to P_{psdA} was almost comparable to the one
414 observed for the P_{bceA} promoter (Fig. 6H). The IM analysis underlying this sensorgram also
415 revealed two binding events, one with fast ON/fast OFF ($k_a=6.2 \times 10^5/\text{M}\cdot\text{s}$; $k_d=1.2 \times 10^{-1}/\text{s}$)
416 and one with slow ON/slow OFF binding kinetics ($k_a=1.1 \times 10^5/\text{M}\cdot\text{s}$; $k_d=6.2 \times 10^{-4}/\text{s}$) likewise
417 resulting in two binding events that differ in their overall affinity ($K_D=188 \text{ nM}$ and $K_D=6.2$
418 nM , respectively). Compared to the affinities of BceR-P to P_{bceA}, the binding affinities for
419 P_{psdA} are indeed in a similar range, but both P_{psdA} binding sites differ in their affinity in the
420 factor of three to BceR-P (Fig. 6L). In agreement with the data obtained for the P_{bceA} promoter
421 region, inactivation of the MBS completely prevented BceR-P binding to the P_{psdA} promoter
422 region (Fig. 6I). Inactivation of the SBS showed a 1:1 interaction described by one peak in the
423 IM analysis that corresponds to the slow ON/slow OFF MBS site with an association rate of
424 $k_a=1.1 \times 10^5 \text{ M}\cdot\text{s}$ and a dissociation rate $k_d=7.3 \times 10^{-4}/\text{s}$ making an overall binding affinity of
425 $K_D=6.7 \text{ nM}$ (Fig. 6M), also fitting well to k_a , k_d , and K_D of the BceR-P/P_{psdA} interaction (Fig.
426 6L). These data clearly demonstrate that the binding mechanism of BceR-P to the P_{psdA}

427 promoter is comparable to that of BceR-P to the P_{bceA} promoter, however, with slightly altered
428 binding kinetics and binding affinities differing by a factor of three.

429 Taken together, the *in vitro* data obtained for the binding of BceR-P to isolated promoter
430 fragments by EMSA (Fig. 5A/B) and SPR spectroscopy (Fig. 6B/E and Fig. 6 H/L) are in
431 good agreement with each other. They indicate a hierarchical cooperative binding of
432 phosphorylated BceR-like RRs first to the MBS and then to the SBS. While promoter
433 discrimination could not be explained by EMSAs alone, we could determine slight differences
434 in the binding affinities by SPR combined with IM analyses that could explain promoter
435 preference and discrimination of isolated RRs on single promoter fragments and therefore
436 selected activation of transcription. Moreover, DNA curvature as well as interaction of BceR-
437 P with the RNA polymerase could be further factors that finally lead to total promoter
438 activation *in vivo*.

439

440 Discussion

441

442 On P_{bceA} and P_{psdA} , no typical -35 element was found in the appropriate location upstream of
443 the -10 element, indicating that the σ unit of the RNA polymerase cannot bind properly to the
444 promoter by itself to initiate transcription initiation. However, binding can nevertheless be
445 established under such conditions when the σ unit interacts with an RR that binds to upstream
446 elements of the promoter, thereby compensating weak σ unit binding (Lee *et al.*, 2012). DNA
447 binding domain structures of both PhoB and OmpR from the OmpR subfamily showed that
448 these RRs can directly interact with the σ subunit of the RNA polymerase (Martínez-Hackert
449 & Stock, 1997, Blanco *et al.*, 2002). BceR and PsdR, which belong to the same subfamily, are
450 assumed to assist the transcription initiation of RNA polymerase in a similar way.

451 Specific transcription initiation by RRs is important for maintaining the insulation of the
452 corresponding signaling systems. The similarity of Bce-like RRs DNA-binding domain and
453 their binding sites on target promoters increases the potential of unwanted cross-talk at the
454 transcription initiation level. However, we could show that Bce-type RRs in *B. subtilis* are
455 extremely specific in inducing the transcription of only their cognate ABC transporter operons.
456 While we observed binding of BceR-P to both the cognate P_{bceA} and the non-cognate P_{psdA}
457 with very similar affinities *in vitro* (Fig. 5A and 5B), BceR can only induce the transcription
458 of *bceAB* but not of *psdAB* *in vivo* (Fig. 3). Moreover, our EMSA experiments showed that
459 when incubated with a mixture of both promoter fragments, BceR is able to specifically bind
460 its cognate target, even if that is present at 30-fold lower concentrations (Fig. 5). Promoter
461 discrimination between cognate and non-cognate binding sites can therefore be based on even
462 minor differences in binding affinities of isolated RRs to the otherwise highly similar binding
463 sites, as demonstrated by the SPR measurements (Fig. 6). This discriminatory ability becomes
464 especially apparent under conditions of competition between binding partners (as shown by
465 the EMSA competition experiments, Fig. 5), which is most reminiscent of the intracellular
466 environment, where both RRs and DNA target sequences are present at the same time.

467 The slight affinity preference is the ability of the RR to distinguish the cognate from non-
468 cognate promoter in the natural cellular setting. Our data strongly suggest that *B. subtilis*
469 evolved a sophisticated mechanism to maintain this ability by combining this existing target
470 site competition of homologous RRs to their respective binding sites with hierarchical and
471 cooperative DNA binding (Fig. 7). Instead of the single binding sites reported previously
472 (Ohki *et al.*, 2003, de Been *et al.*, 2008), we experimentally demonstrated the presence of two
473 binding sites in the regulatory region of the Bce-type RR target promoters (Fig. 2D and 2E),
474 as was already suggested by a comparative genomics study on Bce-like TCSs (Dintner *et al.*,
475 2011). By performing EMSAs and SPR assays of BceR with P_{bceA} mutants carrying random
476 mutation in either the MBS or the SBS, we demonstrated that BceR has a high affinity and

477 shows independent binding to the upstream MBS (Fig. 5C and 6D). BceR has a low affinity
478 for the downstream SBS and cannot bind to it alone under our experimental conditions (Fig.
479 5D and 6C). While it is not possible to unequivocally determine the order of BceR binding to
480 its two target sites from the data presented herein, our results nevertheless strongly suggest
481 that a BceR dimer first binds to the high-affinity MBS. This first binding event might then
482 assist the subsequent binding of another dimer to the downstream low-affinity SBS. In this,
483 binding to the MBS appears to be of low specificity, while the second binding event to the
484 SBS occurs with high specificity. This is supported by our *in vivo* promoter activity assays
485 where we showed that exchanging the SBS between the P_{bceA} and P_{psdA} fragments resulted in a
486 much stronger influence on promoter specificity than exchanging the MBS by *in vivo*
487 promoter activity assays (Fig. 4). This hierarchical and cooperative binding to the two sites
488 enables BceR to discriminate between its cognate promoter P_{bceA} and the non-cognate P_{psdA} ,
489 which is based on: (i) The MBSs of these two promoters differ only in three bases and provide
490 a high-affinity, low-specificity docking site; (ii) The SBSs of these two promoters harbor five
491 different bases and represent low-affinity, yet high specificity interaction sites; (iii) Only this
492 combination of MBS and SBS together with the binding competition described above
493 ultimately allows BceR-P to discriminate between the cognate promoter P_{bceA} and the non-
494 cognate P_{psdA} , thereby ultimately ensuring the wiring specificity of highly similar RRs.

495 It should be pointed out that the specificity of interaction between BceR and the MBS/SBS of
496 either the cognate or non-cognate site – as expressed by the different binding affinities
497 determined by SPR measurement *in vitro* (Fig. 6) – will *in vivo* of course be influenced by the
498 relative cellular concentrations of phosphorylated BceR-like RRs. For both P_{bceA} and P_{psdA} , the
499 K_D values differ by a factor of 30 between the MBS and the SBS, with the first in the range of
500 2-7 nM while the latter was determined in the 50-150 nM range (Fig. 6).

501 The strong discriminatory power of the SBS relative to the MBS suggests cellular BceR-P
502 concentrations in the medium (approx. 10 to 100) nanomolar range. Under such conditions,

503 the MBS of both P_{bceA} and P_{psdA} would be fully bound, while the small differences in binding
504 affinities to the respective SBS should be sufficient for promoter discrimination at RR
505 concentrations near the K_D values. Unfortunately, no data on the cellular concentrations of
506 BceR-like RRs is available, and even a comprehensive quantitative analysis aimed at
507 determining the cellular amounts of all mRNA and protein species of the *B. subtilis* cell failed
508 to detect BceR in any of over 200 conditions tested (Buescher et al. 2012) indicative of a very
509 low basal abundance. The true physiological conditions for promoter-RR interaction therefore
510 have to remain speculative.

511 The linker regions of these two promoters showed characteristically distinct GC/AT contents:
512 P_{bceA} has a high AT content, while P_{psdA} has a high GC content (Fig. 2A). We showed that
513 mutating the linker region into a random sequence while maintaining the GC/AT content of
514 each promoter only slightly affected the promoter activity (Fig. 2D and 2E). However,
515 exchanging the linker region between these two promoters, which means changing the GC/AT
516 content, resulted in a more pronounced effect on the promoter activity (Fig. 4). AT-rich
517 sequences are known to mediate DNA bending (Koo *et al.*, 1986). One possibility is that the
518 AT-rich linker region on P_{bceA} confers a structural difference compared to P_{psdA} by bending the
519 promoter between two binding sites, which might accommodate the binding of two BceR
520 dimers.

521 The high specificity of the SBS is presumably determined mainly by its first half-site, for
522 which P_{bceA} and P_{psdA} differ in four out of seven bases. In contrast, the second half-sites of the
523 SBSs only differ in one base. The sequence identity of the second half-site and its location at
524 the -35 position suggests that it can probably be bound by both BceR and the σ^A subunit of the
525 RNA polymerase. Along those lines, we saw that a P_{bceA} mutant with the SBS replaced by a
526 second MBS (MBS-linker-MBS) completely lost its promoter activity (data not shown),
527 further supporting the importance of the second half for transcription initiation, presumably
528 by σ^A subunit binding. Alternatively, the binding of the σ^{70} subunit to the -35 element could

529 be replaced by protein-protein interactions between the RNA polymerase and BceR/PsdR.
530 Such a mechanism was shown *in vitro* for PhoB and CRP dependent promoter activation.
531 (Kumar *et al.*, 1994). A recent study demonstrated that in PhoB regulated promoters, σ^{70}
532 forms a number contacts with DNA-bound PhoB, replacing contacts with the -35 element
533 (Blanco *et al.*, 2011).

534 Hierarchical and cooperative DNA binding is widespread among the OmpR RR subfamily.
535 For example, PhoB can bind cooperatively to two binding sites in the *pstS* promoter with
536 different individual binding affinities (Blanco *et al.*, 2012). P_{ompF} has three OmpR binding
537 sites with gradually reduced affinity from upstream to downstream, and binding of OmpR to
538 the first site is important for subsequent binding to the lower-affinity downstream sites
539 (Harlocker *et al.*, 1995). Likewise, the RR YpdB from *E. coli* also shows a two-step
540 cooperative binding mechanism to its target promoter P_{yhjX} (Behr *et al.*, 2016): binding of
541 YpdB to the upstream site A initiates subsequent binding to the downstream site B followed
542 by a rapid and successive promoter clearance. Similar to P_{bceA} -binding of BceR, binding of
543 YpdB to P_{yhjX} was completely abolished if site A was inactivated (Behr *et al.*, 2016).

544 Interestingly, highly cooperative binding of BceR-P to its target promoter was already
545 strongly suggested by a recent quantitative study on the regulatory dynamics of the Bce
546 system (Fritz *et al.*, 2015). This study indicated a high degree of cooperativity within the
547 signaling pathway, presumably caused by cooperative binding of BceR-P to multiple sites in
548 the target promoter. This cooperativity was shown to be crucial for the highly dynamic dose-
549 response behavior of *bceAB* expression in the presence of increasing amounts of bacitracin,
550 resulting in an accurate produce-to-demand strategy that adjusts cellular BceAB levels to just
551 the right amount to cope with the current presence of bacitracin (Fritz *et al.*, 2015). These
552 specific results on BceR cooperativity are in good agreement with a recent theoretical study,
553 which identified cooperativity as an important mechanism to significantly reduce crosstalk in
554 gene regulation (Friedlander *et al.*, 2016).

555 The evolution of such complex regulatory mechanisms often correlates with the regulatory
556 function of the RRs: e.g. PhoB and OmpR regulate dozens of operons in *E. coli* in the
557 presence of certain stimuli. Some of these operons need to be highly upregulated while others
558 require only moderate or subtle modulations in response to a given trigger. Controlling such
559 differential expression levels of multiple target operons by a single RR can be achieved
560 through assembly of different numbers of binding sites with sequence variations. We have
561 demonstrated for *B. subtilis* that a similar mechanism can also be used to maintain signaling
562 specificity and regulatory insulation between paralogous Bce-like systems that presumably
563 evolved by gene duplications followed by sequence diversification of both the DNA binding
564 domain and their target promoter sequence. Combining a high-affinity but low-specificity
565 MBS and a high-specificity but low-affinity SBS provides *B. subtilis* with enough sequence
566 space to ensure that Bce-like RRs can evolve the ability to discriminate cognate from non-
567 cognate promoters, thereby ensuring the signaling fidelity of highly paralogous Bce-like
568 systems on the transcription level. It will be interesting to see if such a combination of
569 competitive and hierarchical cooperative binding can also explain the target site
570 discrimination for other paralogous pairs of two-component systems.

571

572 **Experimental procedures**

573

574 ***Bacterial strains and growth conditions.*** All strains used in this study are listed in Table S1.

575 *E. coli* DH5 α and XL1-blue were used for cloning. All *B. subtilis* strains used in this study

576 are derivatives of the laboratory WT strain 168. *E. coli* and *B. subtilis* were grown routinely in

577 Luria-Bertani (LB) medium at 37°C with aeration. *B. subtilis* was transformed by natural

578 competence as previously described (Harwood & Cutting, 1990). Ampicillin (100 $\mu\text{g ml}^{-1}$)

579 was used for selection of all plasmids in *E. coli*. Chloramphenicol (5 $\mu\text{g ml}^{-1}$), spectinomycin

580 (100 $\mu\text{g ml}^{-1}$) or erythromycin (1 $\mu\text{g ml}^{-1}$) plus lincomycin (25 $\mu\text{g ml}^{-1}$) for macrolide-

581 lincosamide-streptogramin B (mls) resistance were used for the selection of *B. subtilis*
582 mutants. Bacitracin was supplied as the Zn²⁺-salt. Growth was measured as optical density at
583 600 nm wavelength (OD₆₀₀). Solid media contained 1.5 % (w/v) agar.

584 **Plasmid construction and genetic techniques.** All plasmids constructed in this study are
585 listed in Table S2. The corresponding primer sequences are provided in the supplemental
586 material (Table S3). Different promoter fragments derived from P_{bceA} and P_{psdA} were fused to
587 *lacZ* and cloned into the vector pAC6 (Stülke *et al.*, 1997) via the EcoRI/BamHI sites. The
588 details of all promoter constructs are given in Table S2. For construction of the BceR-
589 production plasmid in *E. coli*, *bceR* was amplified with primers TM2007/2008 and cloned into
590 vector pET16b with XhoI and BamHI obtaining pCF120, resulting in an N-terminal His₁₀-tag
591 fusion. Constructs for unmarked gene deletion in *B. subtilis* were cloned into the vector
592 pMAD (Arnaud *et al.*, 2004). For each operon to be deleted, 800-1000 bp fragments located
593 immediately before the start codon of the first gene (“up” fragment) and after the stop codon
594 of the last gene (“down” fragment) were amplified. The primers were designed to create a 17-
595 20 bp overlap between the PCR-products (Table S2), facilitating fusion of the fragments by
596 PCR overlap extension and subsequent cloning into pMAD. Gene deletions were performed
597 as previously described (Arnaud *et al.*, 2004). All constructs were checked for by sequencing,
598 and all *B. subtilis* strains created were verified by colony PCR using appropriate primers.

599
600 **β-Galactosidase assays.** Promoter activity assays were performed as described previously
601 (Mascher *et al.*, 2004). In brief, cells were inoculated from fresh overnight cultures and grown
602 in LB medium at 37°C with aeration until they reached an OD₆₀₀ between 0.4 and 0.5. The
603 cultures were split into 2 mL aliquots and challenged with 30 μg ml⁻¹ bacitracin or 2 μg ml⁻¹
604 nisin with one aliquot left untreated (non-induced control). After incubation for an additional
605 30 min at 37°C with aeration, the cultures were harvested and β-galactosidase activities were
606 determined as described previously, with normalization to cell density (Miller, 1972).

607
608 ***Overproduction and purification of His-tagged BceR.*** To produce BceR carrying an N-
609 terminal His₁₀-tag, *E. coli* C43 (DE3) cells harboring plasmid pCF120 were grown at 25 °C
610 with agitation until they reached an OD₆₀₀ of about 0.4. IPTG (0.5 mM) was added to the
611 culture and incubation was continued at 18 °C with agitation overnight. Cells were harvested
612 by centrifugation at 4,400 × g for 10 min. The cell pellet was washed with buffer A (20 mM
613 potassium phosphate buffer [pH7.5], 100 mM NaCl) and stored at -20 °C until use.
614 To purify His₁₀-tagged BceR, cells were resuspended in buffer B (50 mM potassium
615 phosphate buffer [pH 7.5], 500 mM NaCl, 5 mM β-mercapto-ethanol, 10 mM imidazole and
616 10 % (w/v) glycerol) supplemented with 0.1 mM phenylmethylsulfonyl fluoride (PMSF) plus
617 2 mg DNaseI and disrupted by three passages through a French pressure cell (Thermo Fisher)
618 at 20,000 PSI. Unbroken cells were removed by centrifugation at 17,000 × g for 20 min and
619 the cell-free supernatant was filtered through a 0.45 μm syringe filter before loading onto a 1
620 ml Ni²⁺-NTA resin column (Qiagen) pre-equilibrated with 5 column volumes (CVs) of buffer
621 B. Loading was followed by washing with 5 CVs of buffer B and then with 5 CVs of buffer B
622 containing 100 mM imidazole. BceR was eluted with buffer B supplemented with 250 mM
623 imidazole. Fractions containing BceR were pooled and dialyzed in buffer C (50 mM Tris-HCl
624 [pH 7.5], 150 mM NaCl, 10 mM MgSO₄, 5 mM β-mercapto-ethanol, 5 mM imidazole and 10 %
625 (w/v) glycerol) at room temperature for 1 h. Protein concentration was determined with Roti[®]-
626 Nanoquant (Carl Roth), and the proteins stored at 4 °C until use.

627
628 ***Electrophoretic Mobility Shift Assays (EMSA).*** For electrophoretic mobility shift assays,
629 different DNA fragments (around 300bp) generated by PCR using primers TM3146 (5'
630 terminal 6FAM labeled) and TM3137 were purified by gel extraction. Unlabeled DNA
631 fragments were generated by PCR using primers TM3136/3137 and purified by gel extraction.
632 N-terminal His₁₀-BceR samples in the non-phosphorylated state and after phosphorylation
633 with 50 mM phosphoramidate at room temperature for 2 h were centrifuged at 16,060 × g and

634 4 °C for 10 min to remove the aggregated protein. Protein concentrations of the supernatants
635 were determined as above and the proteins were stored on ice. Binding reactions were set by
636 incubating 6FAM-labelled DNA-fragments with different concentrations of His₁₀-BceR at
637 room temperature for 20 min. The reaction mixture included 30 fmol labeled target DNA and
638 0, 0.5, 1.0, 1.5, 2.0 µM protein with binding buffer (20 mM Tris-HCl [pH 7.5], 50 mM KCl,
639 10 mM MgSO₄, 1 mM DTT, 5 µg ml⁻¹ salmon sperm DNA and 4 % (w/v) glycerol) in a total
640 volume of 5.5 µl. Unlabeled competitor DNA was added to the system to a final concentration
641 of 900 fmol. Samples were loaded on a 6% native polyacrylamide gel and electrophoresis was
642 performed by 300 V for 15 min in 1× TBE buffer. 6FAM fluorescence of labeled DNA bands
643 was detected by PhosphorImager (Typhoon Trio™, GE Healthcare).

644

645 ***Surface Plasmon Resonance (SPR) spectroscopy.*** SPR assays were performed in a Biacore
646 T200 using carboxymethyl dextran sensor chips pre-coated with streptavidin (Xantec
647 SAD500-L, XanTec Bioanalytics GmbH, Düsseldorf, Germany). All experiments were
648 carried out at a constant temperature of 25°C and using HBS-EP+ buffer [10 mM HEPES pH
649 7.4; 150 mM NaCl; 3 mM EDTA; 0.05 % (v/v) detergent P20] as running buffer. Before
650 immobilizing the DNA fragments, the chips were equilibrated by three injections using 1 M
651 NaCl/50 mM NaOH at a flow rate of 10 µl min⁻¹. Then, 10 nM of the respective double-
652 stranded biotinylated DNA fragment was injected using a contact time of 420 sec and a flow
653 rate of 10 µl min⁻¹. As a final wash step, 1 M NaCl/50 mM NaOH/50% (v/v) isopropanol was
654 injected. Approximately 100-200 RU of each respective DNA fragment were captured onto
655 the respective flow cell. All interaction kinetics of BceR or BceR-P with the respective DNA
656 fragment were performed in HBS-EP+ buffer at 25°C at a flow rate of 30 µl min⁻¹. The
657 proteins were diluted in HBS-EP+ buffer and passed over all flow cells in different
658 concentrations (0.1 nM-10 nM) using a contact time of 180 sec followed by a 300 sec
659 dissociation time before the next cycle started. After each cycle the surface was regenerated

660 by injection of 2.5 M NaCl for 60 sec at 30 $\mu\text{l min}^{-1}$ flow rate followed by a second
661 regeneration step by injection of 0.5% (w/v) SDS for 60 sec at 30 $\mu\text{l min}^{-1}$. All experiments
662 were performed at 25°C. Sensorgrams were recorded using the Biacore T200 Control
663 software 2.0 and analyzed with the Biacore T200 Evaluation software 2.0. The surface of flow
664 cell 1 was not immobilized with DNA and used to obtain blank sensorgrams for subtraction of
665 bulk refractive index background. The referenced sensorgrams were normalized to a baseline
666 of 0. Peaks in the sensorgrams at the beginning and the end of the injection emerged from the
667 runtime difference between the flow cells of each chip.

668 Calibration-free concentration analysis (CFCA) was performed using a 5 μM solution of
669 purified BceR-P (calculated from Lowry-based protein determination), which was stepwise
670 diluted 1:2, 1:5, 1:10, and 1:20. Each protein dilution was two-time injected, one at 5 $\mu\text{l min}^{-1}$
671 as well as 100 $\mu\text{l min}^{-1}$ flow rate. On the active flow cell P_{psdA} -DNA was used for BceR-P-
672 binding. CFCA basically relies on mass transport, which is a diffusion phenomenon that
673 describes the movement of molecules between the solution and the surface. The CFCA
674 therefore relies on the measurement of the observed binding rate during sample injection
675 under partially or complete mass transport limited conditions. Overall, the initial binding rate
676 (dR/dt) is measured at two different flow rates dependent on the diffusion constant of the
677 protein. The diffusion coefficient of BceR-P was calculated using the Biacore diffusion
678 constant calculator and converter webtool ([https://www.biacore.com/lifesciences/
679 Application_Support/online_support/Diffusion_Coefficient_Calculator/index.html](https://www.biacore.com/lifesciences/Application_Support/online_support/Diffusion_Coefficient_Calculator/index.html)), whereby
680 a globular shape of the protein was assumed. The diffusion coefficient of BceR-P was
681 determined as $D=1.031 \times 10^{-10} \text{ m}^2/\text{s}$. The initial rates of those dilutions that differed in a factor
682 of at least 1.5 were considered for the calculation of the „active“ concentration, which was
683 determined as $5 \times 10^{-8} \text{ M}$ (1% of the total protein concentration determined by Lowry assay) for
684 BceR-P. The quite low percentage of “active” protein compared to total protein does not
685 necessarily mean that most of the protein is inactive due to misfolding and/or aggregation. It

686 is rather possible that not the complete amount is phosphorylated and therefore not “active”
687 and/or that, although thoroughly washed with high salts, a portion of the protein has still DNA
688 bound after the purification process. However, the „active“ protein concentration was
689 ultimately used for calculation of the binding kinetic constants.

690

691 *Interaction map*[®] (IM) analyses

692 IM calculations were performed on the Ridgeview Diagnostic Server (Ridgeview Diagnostics,
693 Uppsala, Sweden). For this purpose, the SPR sensorgrams were exported from the Biacore
694 T200 Evaluation Software 2.0 as *.txt files and imported into TraceDrawer Software 1.5
695 (Ridgeview Instruments, Uppsala, Sweden). IM files were generated using the IM tool within
696 the software, which produces files that were then sent via e-mail to the server
697 (im@ridgeviewdiagnostics.com), where the IM calculations were performed (Altschuk *et al.*
698 2012). The resulting files were then evaluated for spots in the TraceDrawer 1.5 Software, and
699 the IM spots were quantified.

700

701 **Acknowledgements**

702 The authors would like to thank Ainhoa Revilla Guarinos for critical reading of the
703 manuscript and Julia Frunzke for the gift of synthetic phosphoramidate. This work was
704 supported by a grant from the Deutsche Forschungsgemeinschaft (DFG; grant MA2837/1-3 to
705 TM, and Exc114/2 to KJ). CF was supported by a PhD scholarship from the China
706 Scholarship Council. SPR experiments were performed in the Bioanalytics core facility of the
707 LMU Biocenter.

708 **References**

709

710 Altschuh D., Björkelund, H., Strandgård, J., Choulier, L., Malmqvist, M., and Andersson, K. (2012)
711 Deciphering complex protein interaction kinetics using Interaction Map. *Biochem Biophys Res*
712 *Commun* **428**:74-9.

713 Arnaud, M., Chastanet, A., and Débarbouillé, M. (2004) New vector for efficient allelic replacement
714 in naturally nontransformable, low-GC-content, gram-positive bacteria. *Appl Environ*
715 *Microbiol* **70**: 6887-6891.

716 Behr, S., Heermann, R., and Jung, K. (2016) Insights into the DNA-binding mechanism of a LytTR-
717 type transcription regulator. *Biosci Rep* **36**: e00326.

718 Berdy, J. (2005) Bioactive microbial metabolites. *J Antibiot (Tokyo)* **58**: 1-26.

719 Bernard, R., Guiseppi, A., Chippaux, M., Foglino, M., and Denizot, F. (2007) Resistance to bacitracin
720 in *Bacillus subtilis*: unexpected requirement of the BceAB ABC transporter in the control of
721 expression of its own structural genes. *J Bacteriol* **189**: 8636-8642.

722 Blanco, A.G., Canals, A., Bernués, J., Solà, M., and Coll, M. (2011) The structure of a transcription
723 activation subcomplex reveals how sigma70 is recruited to PhoB promoters. *EMBO J* **30**:
724 3776-3785.

725 Blanco, A.G., Canals, A., and Coll, M. (2012) PhoB transcriptional activator binds hierarchically to
726 pho box promoters. *Biol Chem* **393**: 1165-1171.

727 Blanco, A.G., Solà, M., Gomis-Rüth, F.X. and Coll, M. (2002) Tandem DNA recognition by PhoB, a
728 two-component signal transduction transcriptional activator. *Structure* **10**: 701-713.

729 Bourret, R.B. (2010) Receiver domain structure and function in response regulator proteins. *Curr Opin*
730 *Microbiol* **13**: 142-149.

731 Breukink, E., and de Kruijff, B. (2006) Lipid II as a target for antibiotics. *Nat Rev Drug Discov* **5**:
732 321-323.

733 Buescher, J.M., Liebermeister, W., Jules, M., Uhr, M., Muntel, J., Botella, E., et al. (2012) Global
734 network reorganization during dynamic adaptations of *Bacillus subtilis* metabolism. *Science*
735 **335**: 1099-1103.

736 de Been, M., Bart, M.J., Abee, T., Siezen, R.J., and Francke, C. (2008) The identification of response
737 regulator-specific binding sites reveals new roles of two-component systems in *Bacillus*
738 *cereus* and closely related low-GC Gram-positives. *Environ Microbiol* **10**: 2796-2809.

739 Dintner, S., Heermann, R., Fang, C., Jung, K., and Gebhard, S. (2014) A sensory complex consisting
740 of an ATP-binding cassette transporter and a two-component regulatory system controls
741 bacitracin resistance in *Bacillus subtilis*. *J Biol Chem* **289**: 27899-27910.

742 Dintner, S., Staroń, A., Berchtold, E., Petri, T., Mascher, T., and Gebhard, S. (2011) Coevolution of
743 ABC transporters and two-component regulatory systems as resistance modules against
744 antimicrobial peptides in Firmicutes bacteria. *J Bacteriol* **193**: 3851-3862.

745 Fabret, C., Feher, V.A., and Hoch, J.A. (1999) Two-component signal transduction in *Bacillus subtilis*:
746 how one organism sees its world. *J Bacteriol* **181**: 1975-1983.

747 Friedlander, T., Prizak, R., Guet, C.C., Barton, N.H., and Tkacik, G. (2016) Intrinsic limits to gene
748 regulation by global crosstalk. *Nat Commun* **7**: 12307.

749 Fritz, G., Dintner, S., Treichel, N.S., Radeck, J., Gerland, U., Mascher, T., and Gebhard, S. (2015) A
750 new way of sensing: need-based activation of antibiotic resistance by a flux-sensing
751 mechanism. *mBio* **6**: e00975-00915.

752 Galperin, M.Y. (2006) Structural classification of bacterial response regulators: diversity of output
753 domains and domain combinations. *J Bacteriol* **188**: 4169-4182.

754 Galperin, M.Y. (2010) Diversity of structure and function of response regulator output domains. *Curr*
755 *Opin Microbiol* **13**: 150-159.

756 Gao, R., and Stock, A.M. (2009) Biological insights from structures of two-component proteins. *Annu*
757 *Rev Microbiol* **63**: 133-154.

758 Gebhard, S., and Mascher, T. (2011) Antimicrobial peptide sensing and detoxification modules:
759 unravelling the regulatory circuitry of *Staphylococcus aureus*. *Mol Microbiol* **81**: 581-587.

- 760 Grant, S.G., Jessee, J., Bloom, F.R., and Hanahan, D. (1990) Differential plasmid rescue from
761 transgenic mouse DNAs into *Escherichia coli* methylation-restriction mutants. *Proc Natl Acad*
762 *Sci* **87**: 4645-4649.
- 763 Harlocker, S.L., Bergstrom, L., and Inouye, M. (1995) Tandem binding of six OmpR proteins to the
764 ompF upstream regulatory sequence of *Escherichia coli*. *J Biol Chem* **270**: 26849-26856.
- 765 Harwood, C.R., and Cutting, S.M. (1990) *Molecular biological methods for Bacillus*. Chichester: John
766 Wiley and Sons.
- 767 Huynh, T.N., and Stewart, V. (2011) Negative control in two-component signal transduction by
768 transmitter phosphatase activity. *Mol Microbiol* **82**: 275-286.
- 769 Jarmer, H., Larsen, T.S., Krogh, A., Saxild, H.H., Brunak, S., and Knudsen, S. (2001) Sigma A
770 recognition sites in the *Bacillus subtilis* genome. *Microbiology* **147**: 2417-2424.
- 771 Jordan, S., Hutchings, M.I., and Mascher, T. (2008) Cell envelope stress response in Gram-positive
772 bacteria. *FEMS Microbiol Rev* **32**: 107-146.
- 773 Joseph, P., Fichant, G., Quentin, Y., and Denizot, F. (2002) Regulatory relationship of two-component
774 and ABC transport systems and clustering of their genes in the *Bacillus/Clostridium* group,
775 suggest a functional link between them. *J Mol Microbiol Biotechnol* **4**: 503-513.
- 776 Koo, H.-S., Wu, H.-M., and Crothers, D.M. (1986) DNA bending at adenine-thymine tracts. *Nature*
777 **320**: 501-506.
- 778 Kumar, A., B. Grimes, N. Fujita, K. Makino, R.A. Malloch, R.S. Hayward & A. Ishihama, (1994)
779 Role of the sigma 70 subunit of *Escherichia coli* RNA polymerase in transcription activation.
780 *Journal of molecular biology* **235**: 405-413.
- 781 Lee, D.J., Minchin, S.D., and Busby, S.J.W. (2012) Activating transcription in bacteria. *Annu Rev*
782 *Microbiol* **66**: 125-152.
- 783 Martínez-Hackert, E., and Stock, A.M. (1997) The DNA-binding domain of OmpR: crystal structures
784 of a winged helix transcription factor. *Structure* **5**: 109-124.
- 785 Mascher, T., Margulis, N.G., Wang, T., Ye, R.W., and Helmann, J.D. (2003) Cell wall stress
786 responses in *Bacillus subtilis*: the regulatory network of the bacitracin stimulon. *Mol*
787 *Microbiol* **50**: 1591-1604.
- 788 Mascher, T., Zimmer, S.L., Smith, T.A., and Helmann, J.D. (2004) Antibiotic-inducible promoter
789 regulated by the cell envelope stress-sensing two-component system LiaRS of *Bacillus subtilis*.
790 *Antimicrob Agents Chemother* **48**: 2888-2896.
- 791 Miller, J.H. (1972) *Experiments in molecular genetics*. Cold Spring Harbor, New York: Cold Spring
792 Harbor Laboratory Press.
- 793 Miroux, B., and Walker, J.E. (1996) Over-production of proteins in *Escherichia coli*-mutant hosts that
794 allow synthesis of some membrane proteins and globular proteins at high levels. *J Mol Biol*
795 **260**: 289-298.
- 796 Ohki, R., Giyanto, Tateno, K., Masuyama, W., Moriya, S., Kobayashi, K., and Ogasawara, N. (2003)
797 The BceRS two-component regulatory system induces expression of the bacitracin transporter,
798 BceAB, in *Bacillus subtilis*. *Mol Microbiol* **49**: 1135-1144.
- 799 Paget, M., and Helmann, J.D. (2003) The sigma70 family of sigma factors. *Genome Biol* **4**: 203.
- 800 Podgornaia, A.I., and Laub, M.T. (2013) Determinants of specificity in two-component signal
801 transduction. *Curr Opin Microbiol* **16**: 156-162.
- 802 Procaccini, A., Lunt, B., Szurmant, H., Hwa, T., and Weigt, M. (2011) Dissecting the specificity of
803 protein-protein interaction in bacterial two-component signaling: orphans and crosstalks. *PLoS*
804 *ONE* **6**: e19729.
- 805 Rietkötter, E., Hoyer, D., and Mascher, T. (2008) Bacitracin sensing in *Bacillus subtilis*. *Mol*
806 *Microbiol* **68**: 768-785.
- 807 Silver, L.L. (2003) Novel inhibitors of bacterial cell wall synthesis. *Curr Opin Microbiol* **6**: 431-438.
- 808 Staroń, A., Finkeisen, D.E., and Mascher, T. (2011) Peptide antibiotic sensing and detoxification
809 modules of *Bacillus subtilis*. *Antimicrob Agents Chemother* **55**: 515-525.
- 810 Stülke, J., Martin-Verstraete, I., Zagorec, M., Rose, M., Klier, A., and Rapoport, G. (1997) Induction
811 of the *Bacillus subtilis* ptsGHI operon by glucose is controlled by the novel antiterminator,
812 GlcT. *Mol microbiol* **25**: 65-78.

813

814

815

816 **Tables**817 **Table S1.** Bacterial strains used in this study.

Strain	Genotype or characteristic(s) ^a	Reference or source
<i>E. coli</i> strains		
DH5α	<i>recA1 endA1 gyrA96 thi-1 hsdR17</i> (r _K ⁻ m _K ⁺) <i>relA1 glnV44</i> (Grant <i>et al.</i> , 1990) <i>Φ80' ΔlacZ ΔM15 Δ(lacZYA-argF)U169</i>	
XL1-Blue	<i>endA1 gyrA96 (nal^R) thi-1 recA1 relA1 lac supE44</i> [F' <i>proAB⁺ lacI^Δ Δ(lacZ)M15</i>] <i>hsdR17</i> (r _K ⁻ m _K ⁺)	Stratagene
C43 (DE3)	F ⁻ <i>ompT gal dcm hsdS_B</i> (r _B ⁻ m _B ⁻)(DE3)	(Miroux & Walker, 1996)
<i>B. subtilis</i> strains		
W168	Wild type, <i>trpC2</i>	Laboratory stock
TMB279	W168 <i>amyE::pER603</i> ; cm ^r	(Rietkötter <i>et al.</i> , 2008)
TMB299	W168 <i>amyE::pER605</i> ; cm ^r	(Rietkötter <i>et al.</i> , 2008)
TMB412	W168 <i>amyE::pCF601</i> ; cm ^r	This study
TMB607	W168 <i>amyE::pJS605</i> ; cm ^r	This study
TMB805	W168 <i>amyE::pAS601</i> ; cm ^r	This study
TMB806	W168 <i>amyE::pAS602</i> ; cm ^r	This study
TMB960	W168 <i>amyE::pAS603</i> ; cm ^r	This study
TMB961	W168 <i>amyE::pAS604</i> ; cm ^r	This study
TMB962	W168 <i>amyE::pAS605</i> ; cm ^r	This study
TMB963	W168 <i>amyE::pAS606</i> ; cm ^r	This study
TMB964	W168 <i>amyE::pAS607</i> ; cm ^r	This study
TMB965	W168 <i>amyE::pAS608</i> ; cm ^r	This study
TMB966	W168 <i>amyE::pAS609</i> ; cm ^r	This study
TMB967	W168 <i>amyE::pAS610</i> ; cm ^r	This study
TMB1047	W168 <i>amyE::pAS613</i> ; cm ^r	This study
TMB1048	W168 <i>amyE::pAS614</i> ; cm ^r	This study
TMB1049	W168 <i>amyE::pAS615</i> ; cm ^r	This study
TMB1050	W168 <i>amyE::pAS616</i> ; cm ^r	This study
TMB1051	W168 <i>amyE::pAS617</i> ; cm ^r	This study
TMB1052	W168 <i>amyE::pAS618</i> ; cm ^r	This study
TMB1053	W168 <i>amyE::pAS619</i> ; cm ^r	This study
TMB1054	W168 <i>amyE::pAS620</i> ; cm ^r	This study
TMB1460	W168 with unmarked deletions of the <i>bceRS</i> loci	This study
TMB1462	W168 with unmarked deletions of the <i>psdRS</i> loci	This study
TMB2244	W168 <i>amyE::pMG600</i> ; cm ^r	This study
TMB2245	W168 <i>amyE::pMG601</i> ; cm ^r	This study
TMB2247	W168 <i>amyE::pMG603</i> ; cm ^r	This study
TMB2248	W168 <i>amyE::pMG604</i> ; cm ^r	This study
TMB2249	W168 <i>amyE::pMG605</i> ; cm ^r	This study
TMB2250	W168 <i>amyE::pMG606</i> ; cm ^r	This study
TMB2252	W168 <i>amyE::pMG608</i> ; cm ^r	This study
TMB2253	W168 <i>amyE::pMG609</i> ; cm ^r	This study
TMB2303	TMB1462 <i>amyE::pER603</i> ; cm ^r	This study
TMB2304	TMB1462 <i>amyE::pCF601</i> ; cm ^r	This study
TMB2307	TMB1460 <i>amyE::pER603</i> ; cm ^r	This study
TMB2308	TMB1460 <i>amyE::pCF601</i> ; cm ^r	This study
TMB2382	TMB1460 <i>amyE::pMG600</i> ; cm ^r	This study
TMB2383	TMB1460 <i>amyE::pMG601</i> ; cm ^r	This study
TMB2385	TMB1460 <i>amyE::pMG603</i> ; cm ^r	This study
TMB2386	TMB1460 <i>amyE::pMG604</i> ; cm ^r	This study
TMB2387	TMB1462 <i>amyE::pMG600</i> ; cm ^r	This study

TMB2388	TMB1462 <i>amyE</i> ::pMG601; cm ^r	This study
TMB2390	TMB1462 <i>amyE</i> ::pMG603; cm ^r	This study
TMB2391	TMB1462 <i>amyE</i> ::pMG604; cm ^r	This study
TMB2392	TMB1460 <i>amyE</i> ::pMG605; cm ^r	This study
TMB2393	TMB1460 <i>amyE</i> ::pMG606; cm ^r	This study
TMB2395	TMB1460 <i>amyE</i> ::pMG608; cm ^r	This study
TMB2396	TMB1460 <i>amyE</i> ::pMG609; cm ^r	This study
TMB2397	TMB1462 <i>amyE</i> ::pMG606; cm ^r	This study
TMB2399	TMB1462 <i>amyE</i> ::pMG608; cm ^r	This study
TMB2400	TMB1462 <i>amyE</i> ::pMG609; cm ^r	This study
TMB2455	W168 <i>amyE</i> ::pMG612; cm ^r	This study
TMB2456	W168 <i>amyE</i> ::pMG613; cm ^r	This study
TMB2457	W168 <i>amyE</i> ::pMG614; cm ^r	This study
TMB2460	W168 <i>amyE</i> ::pMG617; cm ^r	This study
TMB2461	W168 <i>amyE</i> ::pMG618; cm ^r	This study
TMB2462	W168 <i>amyE</i> ::pMG619; cm ^r	This study
TMB2463	TMB1462 <i>amyE</i> ::pMG614; cm ^r	This study
TMB2464	TMB1460 <i>amyE</i> ::pMG614; cm ^r	This study
TMB2465	TMB1462 <i>amyE</i> ::pMG613; cm ^r	This study
TMB2466	TMB1460 <i>amyE</i> ::pMG613; cm ^r	This study
TMB2467	TMB1462 <i>amyE</i> ::pMG619; cm ^r	This study
TMB2468	TMB1460 <i>amyE</i> ::pMG619; cm ^r	This study
TMB2469	TMB1462 <i>amyE</i> ::pMG618; cm ^r	This study
TMB2470	TMB1460 <i>amyE</i> ::pMG618; cm ^r	This study
TMB2475	TMB1462 <i>amyE</i> ::pMG605; cm ^r	This study
TMB2505	W168 <i>amyE</i> ::pCF608; cm ^r	This study
TMB2506	W168 <i>amyE</i> ::pCF609; cm ^r	This study
TMB2507	W168 <i>amyE</i> ::pCF610; cm ^r	This study
TMB2508	W168 <i>amyE</i> ::pCF611; cm ^r	This study
TMB2509	W168 <i>amyE</i> ::pMG621; cm ^r	This study
TMB2510	TMB1460 <i>amyE</i> ::pMG621; cm ^r	This study
TMB2511	TMB1462 <i>amyE</i> ::pMG621; cm ^r	This study
TMB2512	W168 <i>amyE</i> ::pMG622; cm ^r	This study
TMB2513	TMB1460 <i>amyE</i> ::pMG622; cm ^r	This study
TMB2514	TMB1462 <i>amyE</i> ::pMG622; cm ^r	This study
TMB2515	W168 <i>amyE</i> ::pCF612; cm ^r	This study
TMB2516	TMB1460 <i>amyE</i> ::pCF612; cm ^r	This study
TMB2517	TMB1462 <i>amyE</i> ::pCF612; cm ^r	This study
TMB2518	W168 <i>amyE</i> ::pCF613; cm ^r	This study
TMB2519	TMB1460 <i>amyE</i> ::pCF613; cm ^r	This study
TMB2520	TMB1462 <i>amyE</i> ::pCF613; cm ^r	This study
TMB2536	W168 <i>amyE</i> ::pCF614; cm ^r	This study
TMB2537	TMB1460 <i>amyE</i> ::pCF614; cm ^r	This study
TMB2538	TMB1462 <i>amyE</i> ::pCF614; cm ^r	This study
TMB2539	W168 <i>amyE</i> ::pCF615; cm ^r	This study
TMB2540	TMB1460 <i>amyE</i> ::pCF615; cm ^r	This study
TMB2541	TMB1462 <i>amyE</i> ::pCF615; cm ^r	This study
TMB2631	W168 <i>amyE</i> ::pCF616	This study
TMB2632	TMB1460 <i>amyE</i> ::pCF616	This study
TMB2633	TMB1462 <i>amyE</i> ::pCF616	This study
TMB2637	W168 <i>amyE</i> ::pCF618	This study
TMB2638	TMB1460 <i>amyE</i> ::pCF618	This study
TMB2639	TMB1462 <i>amyE</i> ::pCF618	This study
TMB2640	W168 <i>amyE</i> ::pCF619; cm ^r	This study
TMB2641	TMB1460 <i>amyE</i> ::pCF619; cm ^r	This study
TMB2642	TMB1462 <i>amyE</i> ::pCF619; cm ^r	This study
TMB2643	W168 <i>amyE</i> ::pCF620; cm ^r	This study
TMB2644	TMB1460 <i>amyE</i> ::pCF620; cm ^r	This study
TMB2645	TMB1462 <i>amyE</i> ::pCF620; cm ^r	This study

819 **Table S2.** Vectors and plasmids used in this study.

Plasimd	Genotype or characteristic(s)	Primers used for cloning	Reference or source
Vectors			
pAC6	Vector for transcriptional promoter fusions to <i>lacZ</i> in <i>B. subtilis</i> , integrates in <i>amyE</i> ; <i>cm^r</i>		(Stülke <i>et al.</i> , 1997)
pET16b	Vector for IPTG-inducible gene expression; carries a N-terminal His ₁₀ -tag sequence; <i>amp^r</i>		Novagen
pMAD	Vector for construction of unmarked deletions in <i>B. subtilis</i> , temperature sensitive replicon; <i>mls^r</i>		(Arnaud <i>et al.</i> , 2004)
Plasmids			
pAS601	pAC6 P _{<i>psdA</i>} (-99 to +30) - <i>lacZ</i>	1591/0600	This study
pAS602	pAC6 P _{<i>psdA</i>} (-97 to +30) - <i>lacZ</i>	1592/0600	This study
pAS603	pAC6 P _{<i>psdA</i>} (-104 to +30) - <i>lacZ</i>	1688/0600	This study
pAS604	pAC6 P _{<i>psdA</i>} (-103 to +30) - <i>lacZ</i>	1687/0600	This study
pAS605	pAC6 P _{<i>psdA</i>} (-102 to +30) - <i>lacZ</i>	1686/0600	This study
pAS606	pAC6 P _{<i>psdA</i>} (-101 to +30) - <i>lacZ</i>	1685/0600	This study
pAS607	pAC6 P _{<i>psdA</i>} (-100 to +30) - <i>lacZ</i>	1684/0600	This study
pAS608	pAC6 P _{<i>psdA</i>} (-98 to +30) - <i>lacZ</i>	1683/0600	This study
pAS609	pAC6 P _{<i>psdA</i>} (-96 to +30) - <i>lacZ</i>	1682/0600	This study
pAS610	pAC6 P _{<i>psdA</i>} (-95 to +30) - <i>lacZ</i>	1681/0600	This study
pAS613	pAC6 P _{<i>bceA</i>} (-110 to +82) - <i>lacZ</i>	1869/0555	This study
pAS614	pAC6 P _{<i>bceA</i>} (-109 to +82) - <i>lacZ</i>	1870/0555	This study
pAS615	pAC6 P _{<i>bceA</i>} (-108 to +82) - <i>lacZ</i>	1871/0555	This study
pAS616	pAC6 P _{<i>bceA</i>} (-107 to +82) - <i>lacZ</i>	1872/0555	This study
pAS617	pAC6 P _{<i>bceA</i>} (-106 to +82) - <i>lacZ</i>	1873/0555	This study
pAS618	pAC6 P _{<i>bceA</i>} (-105 to +82) - <i>lacZ</i>	1874/0555	This study
pAS619	pAC6 P _{<i>bceA</i>} (-104 to +82) - <i>lacZ</i>	1875/0555	This study
pAS620	pAC6 P _{<i>bceA</i>} (-103 to +82) - <i>lacZ</i>	1876/0555	This study
pCF101	pMAD Δ <i>bceRS</i>	2351/2352 2353/2354	This study
pCF103	pMAD Δ <i>psdRS</i>	2357/2358 2359/2360	This study
pCF120	pET16b <i>bceR</i>	2007/2008	This study
pCF601	pAC6 P _{<i>psdA</i>} (-126 to +30) - <i>lacZ</i>	0674/0600	This study
pCF608	pAC6 P _{<i>bceA</i>} (-122 to +82) main binding site mutation- <i>lacZ</i>	2262/3563 3564/0555	This study
pCF609	pAC6 P _{<i>bceA</i>} (-122 to +82) second binding site mutation- <i>lacZ</i>	0554/3565 3566/0555	This study
pCF610	pAC6 P _{<i>psdA</i>} (-126 to +30) main binding site mutation- <i>lacZ</i>	2262/3567 3568/0600	This study
pCF611	pAC6 P _{<i>psdA</i>} (-126 to +30) second binding site mutation- <i>lacZ</i>	0674/3569 3570/0600	This study
pCF612	pAC6 P _{<i>psdA</i>} (-126 to +30) second binding site switched into the corresponding region of P _{<i>bceA</i>} - <i>lacZ</i>	0674/3553 3554/0600	This study
pCF613	pAC6 P _{<i>psdA</i>} (-126 to +30) linker and second binding site switched into the corresponding region of P _{<i>bceA</i>} - <i>lacZ</i>	0674/3557 3558/0600	This study
pCF614	pAC6 P _{<i>bceA</i>} (-122 to +82) main binding site, linker and second binding site switched into the corresponding region of P _{<i>psdA</i>} - <i>lacZ</i>	3692/0555	This study
pCF615	pAC6 P _{<i>psdA</i>} (-126 to +30) main binding site, linker and second binding site switched into the corresponding region of P _{<i>bceA</i>} - <i>lacZ</i>	3693/0600	This study
pCF616	pAC6 P _{<i>bceA</i>} (-122 to +82) main binding site and second binding site switched into the corresponding region of P _{<i>psdA</i>} - <i>lacZ</i>	3719/0555	This study

pCF618	pAC6 P _{bceA} (-122 to +82) main binding site and linker switched into the corresponding region of P _{psdA} -lacZ	3721/0555	This study
pCF619	pAC6 P _{psdA} (-126 to +30) main binding site and second binding site switched into the corresponding region of P _{bceA} -lacZ	3720/0600	This study
pCF620	pAC6 P _{psdA} (-126 to +30) main binding site and linker switched into the corresponding region of P _{bceA} -lacZ	3722/0600	This study
pER603	pAC6 P _{bceA} (-122 to +82) -lacZ	0554/0555	(Rietkötter <i>et al.</i> , 2008)
pER605	pAC6 P _{psdA} (-110 to +30) -lacZ	0599/0600	(Rietkötter <i>et al.</i> , 2008)
pMG600	pAC6 P _{bceA} (-122 to -46) - P _{psdA} (-36 to +30) (BP1) -lacZ	1689/3240 3241/0600	This study
pMG601	pAC6 P _{bceA} (-122 to -56) - P _{psdA} (-46 to +30) (BP2) -lacZ	1689/3242 3243/0600	This study
pMG603	pAC6 P _{bceA} (-122 to -76) - P _{psdA} (-66 to +30) (BP3) -lacZ	1689/3246 3247/0600	This study
pMG604	pAC6 P _{bceA} (-122 to -88) - P _{psdA} (-79 to +30) (BP4) -lacZ	1689/3248 3249/0600	This study
pMG605	pAC6 P _{psdA} (-126 to -37) - P _{bceA} (-45 to +82) (PB1) -lacZ	0674/3230 3231/0555	This study
pMG606	pAC6 P _{psdA} (-126 to -47) - P _{bceA} (-55 to +82) (PB2) -lacZ	0674/3232 3233/0555	This study
pMG608	pAC6 P _{psdA} (-126 to -67) - P _{bceA} (-75 to +82) (PB3) -lacZ	0674/3236 3237/0555	This study
pMG609	pAC6 P _{psdA} (-126 to -80) - P _{bceA} (-87 to +82) (PB4) -lacZ	0674/3238 3239/0555	This study
pMG612	pAC6 P _{bceA} (-122 to + 82) linker mutation - lacZ	0146/3351 3395/0010	This study
pMG613	pAC6 P _{bceA} (-122 to + 82) linker switched into the corresponding part of P _{psdA} -lacZ	0146/3401 3400/0010	This study
pMG614	pAC6 P _{bceA} (-122 to + 82) main binding site switched into the corresponding region of P _{psdA} -lacZ	0146/3419 3354/0010	This study
pMG617	pAC6 P _{psdA} (-126 to + 30) linker mutation - lacZ	0146/3353 3352/0600	This study
pMG618	pAC6 P _{psdA} (-126 to + 30) linker switched into the corresponding region of P _{bceA} -lacZ	0146/3403 3402/0600	This study
pMG619	pAC6 P _{psdA} (-126 to + 30) main binding site switched into the corresponding region of P _{bceA} -lacZ	0146/3357 3356/0600	This study
pMG621	pAC6 P _{bceA} (-122 to + 82) second binding site switched into the corresponding region of P _{psdA} -lacZ	2262/3551 3552/0555	This study
pMG622	pAC6 P _{bceA} (-122 to + 82) linker and the second binding site switched into the corresponding region of P _{psdA} -lacZ	2262/3555 3556/0555	This study
pJS605	pAC6 P _{bceA} (-111 to +82) -lacZ	1307/0555	This study

820 Amp, ampicillin; cm, chloramphenicol; mls, macrolide-lincosamide-streptogramin B group antibiotics; r,
821 resistant.

822

823 Supplemental Table S3. Primers used in this study.

Primer name	Sequence (5'-3') ^a	Use
TM0010	CTTCGCTATTACGCCAGCTGG	<i>lacZ</i> check rev
TM0146	GTCTGCTTTCTCATTAGAATCAATCC	<i>cat</i> check rev
TM0554	GATCGAATTCGAACATGTCATAAGCGTGTGACG	<i>P_{bceA}</i> (-122) fwd
TM0555	GATCGGATCCATCGATGCCCTCAGCACTTCC	<i>P_{bceA}</i> rev
TM0599	AGTCGAATTCACCCTCGTGAATGTGACAGC	<i>P_{psdA}</i> (-110) fwd
TM0600	AGTCGGATCCCGATAGGTTTCGTTGTTGCAACACG	<i>P_{psdA}</i> rev
TM0674	AGTCGAATTCCTCGTGTTCCTCAAGTGACACC	<i>P_{psdA}</i> (-126) fwd
TM1307	GATCGAATTCGAAGCGTGTGACGAAAATGTCACAT	<i>P_{bceA}</i> (-111) fwd
TM1591	AGTCGAATTCATGTGACAGCATTGTAAGATTGG	<i>P_{psdA}</i> (-99) fwd
TM1592	AGTCGAATTCGTGACAGCATTGTAAGATTGG	<i>P_{psdA}</i> (-97) fwd
TM1681	AGTCGAATTCACGACAGCATTGTAAGATTGG	<i>P_{psdA}</i> (-95) fwd
TM1682	AGTCGAATTCATGACAGCATTGTAAGATTGG	<i>P_{psdA}</i> (-96) fwd
TM1683	AGTCGAATTCGTGACAGCATTGTAAGATTGG	<i>P_{psdA}</i> (-98) fwd
TM1684	AGTCGAATTCATGACAGCATTGTAAG	<i>P_{psdA}</i> (-100) fwd
TM1685	AGTCGAATTCGAATGTGACAGCATTGTAAG	<i>P_{psdA}</i> (-101) fwd
TM1686	AGTCGAATTCATGACAGCATTGTAAG	<i>P_{psdA}</i> (-102) fwd
TM1687	AGTCGAATTCAGTGAATGTGACAGCATTGTAAG	<i>P_{psdA}</i> (-103) fwd
TM1688	AGTCGAATTCGGTGAATGTGACAGCATTGTAAG	<i>P_{psdA}</i> (-104) fwd
TM1689	CCGATGATAAGCTGTCAAAC	pAC6 bandshifts
TM1869	ATGCGAATTCAGCGTGTGACGAAAATG	<i>P_{bceA}</i> (-110) fwd
TM1870	ATGCGAATTCGCGTGTGACGAAAATGTC	<i>P_{bceA}</i> (-109) fwd
TM1871	ATGCGAATTCACGTGTGACGAAAATGTC	<i>P_{bceA}</i> (-108) fwd
TM1872	ATGCGAATTCAGTGTGACGAAAATGTC	<i>P_{bceA}</i> (-107) fwd
TM1873	ATGCGAATTCAAAATGTGACGAAAATGTC	<i>P_{bceA}</i> (-106) fwd
TM1874	ATGCGAATTCGTGACGAAAATGTCAC	<i>P_{bceA}</i> (-105) fwd
TM1875	ATGCGAATTCATGACGAAAATGTCAC	<i>P_{bceA}</i> (-104) fwd
TM1876	ATGCGAATTCAGACGAAAATGTCAC	<i>P_{bceA}</i> (-103) fwd
TM2007	ATCGCTCGAGTTGTTTAAACTTTTGCTGATTG	<i>bceR</i> rev
TM2008	ATCGGGATCCCTTAATCATAGAACTTGTCCCTC	<i>bceR</i> rev
TM2262	GAGCGTAGCGAAAAATCC	pAH328 checkfwd
TM2351	AATTTGGATCCGAGGAAGCAAAAAGGAAATC	<i>bceRS</i> deletion up fwd
TM2352	CTTGATTTTCATGAAACAGCG	<i>bceRS</i> deletion up rev
TM2353	ctgtttcatgaaatcaag ATATTGATGTTGAGTCGGAG	<i>bceRS</i> deletion down fwd
TM2354	AATTCATGGTTCAAATTTTCGAGGATGAG	<i>bceRS</i> deletion down rev
TM2357	AATTTGGATCCCTACGATCTAAAATGGTTTCC	<i>psdRS</i> deletion up fwd
TM2358	ATTTTTGAAGATGACCGCCC	<i>psdRS</i> deletion up rev
TM2359	cgttcattctcaaaa CACTGTGATGACCATCGTG	<i>psdRS</i> deletion down fwd
TM2360	AATTCATGGACCGAAACGGCAAAACACAC	<i>psdRS</i> deletion down rev
TM3230	GTCAGCATCCTCCCATCGAAC	PB1 up rev
TM3231	cgatggaggatgctgac TTCCTTTTATAATGAGATTATCC	PB1 down fwd
TM3232	TCCCATCGAACTTTCTTGCAATTC	PB2 up rev
TM3233	caagaaagtctgatggga AAGCCCGGCATTCCTTTTATAATG	PB2 down fwd
TM3236	TCCCCTCCCCAATCTTACAATG	PB3 up rev
TM3237	taagattggggagcggaa TTGTTCCCGTATCGAAGG	PB3 down fwd
TM3238	ATCTTACAATGCTGTCACATTC	PB4 up rev
TM3239	gtgacagcattgtaagat GCTTTTCTTTTTGTTTCGCCG	PB4 down fwd
TM3240	TGCCGGCTTTTCCTTCGATAC	BP1 up rev
TM3241	cgaaggaaaagccggcaTTCCTTTTATAATAAAGAAAAAGG	BP1 down fwd
TM3242	TTCCTTCGATACGGCGAAC	BP2 up rev
TM3243	ttccgctatcgaaggaaGGATGCTGACTTCCTTTTATAATAAAG	BP2 down fwd
TM3246	AAAAGAAAAGCATGTGACATTTTC	BP3 up rev
TM3247	gtcacatctttcttttTGCAAGAAAGTTCGATGGGAGG	BP3 down fwd
TM3248	ATGTGACATTTTCGTCACACGC	BP4 up rev
TM3249	gtgacgaaaatgtcacatTGGGGAGCGGAATTGCAAGAAAG	BP4 down fwd
TM3351	cgaacaaattgtataGCATGTGACATTTTCGTC	<i>P_{bceA}</i> L-M up rev
TM3352	cgacggcaattgcaAGAAAGTTCGATGGGAGG	<i>P_{psdA}</i> L-M down fwd
TM3353	tgaattgcccgtgcaCAATCTTACAATGCTGTCAC	<i>P_{psdA}</i> L-M up rev
TM3354	gacagcattgtaagaTGCTTTTCTTTTTGTTTCGCC	<i>P_{bceA}</i> M-S down fwd
TM3356	gacgaaaatgtcacaTTGGGGAGCGGAATTGCAAG	<i>P_{psdA}</i> M-S down fwd
TM3357	tgtgacatttctgcaACATTCACGAGGGTGTCACTTG	<i>P_{psdA}</i> M-S up rev
TM3395	tatacaaatgttctcCCGTATCGAAGGAAAAAGC	<i>P_{bceA}</i> L-M down fwd
TM3400	ggcgaacaatccgctcccGCATGTGACATTTTCGTCAC	<i>P_{bceA}</i> L-S down fwd

TM3401	gggagcggattgttcgccGTATCGAAGG	P_{bceA} L-S up rev
TM3402	cttgcaataaaagaaaaCAATCTTACAATGCTGTCCAC	P_{psdA} L-S down fwd
TM3403	tttttttattgcaagAAAGTTTCGATGGG	P_{psdA} L-S up rev
TM3419	tcttacaatgctgtcACACGCTTATGACATGTTCG	P_{bceA} M-S up rev
TM3551	ccatcgaaatttttgCAAAAAAGAAAAGCATGTGACATTTTC	P_{bceA} S-S up rev
TM3552	caagaaagtctgatGGAAAAGCCCGGCATTCC	P_{bceA} S-S down fwd
TM3553	ccttcgatacggcgaaCAATTCGCTCCCAATC	P_{psdA} S-S up rev
TM3554	ttcgccgatacgaaGGGAGGATGCTGACTTCC	P_{psdA} S-S down fwd
TM3555	actttttgcaattccgctccccaATGTGACATTTTCGTCCACACG	P_{bceA} S+L-S up rev
TM3556	ggaattgcaagaaagtctgatGGAAAAGCCCGGCATTCC	P_{bceA} S+L-S down fwd
TM3557	tacggcgaacaaaaagaaaaATCTTACAATGCTGTCCACATTC	P_{psdA} S+L-S up rev
TM3558	ttttttgttcgctatcgaaGGGAGGATGCTGACTTCC	P_{psdA} S+L-S down fwd
TM3563	gcgttaagtaccgctaaCGCTTATGACATGTTTCGAATTCCG	P_{bceA} M-M up rev
TM3564	ttageggtgactaacgcTGCTTTTCTTTTTTGTTCGCCG	P_{bceA} M-M down fwd
TM3565	cagctagcagctcagAAAAAGAAAAGCATGTGACATTTTC	P_{bceA} S-M up rev
TM3566	ctgactgactgactgAAAAAGCCCGGCATTTCCTTTT	P_{bceA} S-M down fwd
TM3567	tacttcggtcaccgctaaTTCACGAGGTTGCTCACTTG	P_{psdA} M-M up rev
TM3568	ttagcggtagccgaagtaTTGGGAGCGGAATTGCAAG	P_{psdA} M-M down fwd
TM3569	gtcagtcgctcagcagcATTCCGCTCCCAATCTTAC	P_{psdA} S-M up rev
TM3570	gactgactgactgactgAGGATGCTGACTTTCCTTTT	P_{psdA} S-M down fwd
TM3665	GTCATAAGCGTGTGACGAAAATGTCACATGCTTTTCTTTTTTGTTC GCCGTATCGAAGGAAAAGCCCGGCATTCCCT	P_{bceA} WT fwd (for SPR)
TM3666	AGGAATGCCGGGCTTTTCCTTCGATACGGCGAACAAAAAGAAA AGCATGTGACATTTTCGTCCACACGCTTATGAC	Biotin- P_{bceA} WT rev (for SPR)
TM3667	CCCTCGTGAATGTGACAGCATTGTAAGATTGGGGAGCGGAATTG CAAGAAAGTTCGATGGGAGGATGCTGACTTCCT	P_{psdA} WT fwd (for SPR)
TM3668	AGGAAGTCAGCATCCTCCCATCGAACTTTCTTGCAATTCGCTCC CCAATCTTACAATGCTGTCCACATTCACGAGGG	Biotin- P_{psdA} WT rev (for SPR)
TM3669	GTCATAAGCGTTAGCGGTGACTTAAACGCTGCTTTTCTTTTTTGTTC GCCGTATCGAAGGAAAAGCCCGGCATTCCCT	P_{bceA} M-M fwd (for SPR)
TM3670	AGGAATGCCGGGCTTTTCCTTCGATACGGCGAACAAAAAGAAA AGCAGCGTTAAGTCACCGCTAACGCTTATGAC	Biotin- P_{bceA} M-M rev (for SPR)
TM3671	CCCTCGTGAATTAGCGGTGACCGAAGTATTGGGGAGCGGAATTG CAAGAAAGTTCGATGGGAGGATGCTGACTTCCT	P_{psdA} M-M fwd (for SPR)
TM3672	AGGAAGTCAGCATCCTCCCATCGAACTTTCTTGCAATTCGCTCC CCAATACTTCGGTCACCGCTAATTCACGAGGG	Biotin- P_{psdA} M-M rev (for SPR)
TM3673	GTCATAAGCGTGTGACGAAAATGTCACATGCTTTTCTTTTTTCTGA CTGACTGCTAGCTGAAAAGCCCGGCATTCCCT	P_{bceA} S-M fwd (for SPR)
TM3674	AGGAATGCCGGGCTTTTCAGCTAGCAGTCAGAAAAAGAAA AGCATGTGACATTTTCGTCCACACGCTTATGAC	Biotin- P_{bceA} S-M rev (for SPR)
TM3675	CCCTCGTGAATGTGACAGCATTGTAAGATTGGGGAGCGGAATGA CTGACTGACGACTGACGAGGATGCTGACTTCCT	P_{psdA} S-M fwd (for SPR)
TM3676	AGGAAGTCAGCATCCTCGTCAGTCAGTCAGTCATTCCGCTCC CCAATCTTACAATGCTGTCCACATTCACGAGGG	Biotin- P_{psdA} S-M rev (for SPR)
TM3677	TCACGAATTACCATCTACACCCTGCCAAAAATTTGATAAACTTAT TTTATAAAAAAATTGAAACCTTTTGAACGAA	P_{sigW} WT fwd (for SPR)
TM3678	TTCGTTTTCAAAGGTTTCAATTTTTTTATAAAATAAGTTTATCAAA TTTTTGGCAGGGTGTAGATGGTAATTCGTGA	Biotin- P_{sigW} WT rev (for SPR)
TM3692	GATCGAATTCGAACATGTCATAAGCGTGTGACAGCATTGTAAGA TTGGGGAGCGGAATTGC	P_{bceA} M+L+S-S fwd
TM3693	AGTCGAATTCCTCGTGTTCCTCAAGTGACACCCTCGTGAATGTGACG AAAATGTCACATGCTTTTCTTTTTTGTTCGC	P_{psdA} M+L+S-S fwd
TM3719	GATCGAATTCGAACATGTCATAAGCGTGTGACAGCATTGTAAGA TGCTTTTCTTTTTTGAAG	P_{bceA} M+S-S fwd
TM3720	AGTCGAATTCCTCGTGTTCCTCAAGTGACACCCTCGTGAATGTGACG AAAATGTCACATTCGGGGAGCGGAATTG	P_{psdA} M+S-S fwd
TM3721	GATCGAATTCGAACATGTCATAAGCGTGTGACAGCATTGTAAGA TTG	P_{bceA} M+L-S fwd
TM3722	AGTCGAATTCCTCGTGTTCCTCAAGTGACACCCTCGTGAATGTGACG AAAATGTCACATG	P_{psdA} M+L-S fwd

824

^a Restriction sites are underlined; overlaps to other primers for PCR fusions are shown by lower case letters.

825 **Figure legends**

826

827 **Figure 1. Model of signal transduction pathways of two Bce-like systems after induction**828 **with corresponding AMPs in *Bacillus subtilis*.** The TCSs Bce and Psd and their inducing

829 antibiotics as signal inputs are highlighted black and grey, respectively. For reasons of

830 simplicity, the ABC transporters of both systems are not shown. Solid arrows indicate the

831 signal transduction pathway within one system, while cross-regulation between BceS and

832 PsdR is highlighted by the dotted arrow. On each promoter, MBS representing for the main

833 binding site and SBS representing for the secondary binding of Bce-like RRs are filled with

834 white on *bceA* promoter and slashes on *psdA* promoter. CM, cell membrane.

835

836 **Figure 2. Functional analysis of *bceA* and *psdA* promoters of *B. subtilis*.** (A) DNA837 sequence alignment of the *bceA* promoter and the *psdA* promoter. Different motifs are framed

838 and annotated underneath the DNA sequence. Important positions on each promoter are

839 marked with arrows according to the start codon of the corresponding regulated gene. Half

840 binding sites of Bce-like RRs on each promoter are emphasized in bold face. Activities of (B)

841 truncated constructions of the *bceA* promoter (from -122: +82 to -103: +82) and (C) truncated842 constructions of the *psdA* promoter (from -126: +30 to -95: +30) according to the start codon843 of regulated genes. Activities of (D) P_{*bceA*} mutants and (E) P_{*psdA*} mutants with MBS^R (main844 binding site random mutation), L^R (linker random mutation) and SBS^R (secondary binding site

845 random mutation) are compared with the corresponding WT promoters. All promoter

846 constructions were fused to *lacZ* and introduced into *amyE* locus of *B. subtilis* 168. Cultures847 growing exponentially in LB were challenged with Zn²⁺-bacitracin 30 µg ml⁻¹ (black bars) or848 nisin 2 µg ml⁻¹ (grey bars) for 30 min, comparing with the non-induced condition (white bars).

849 β-galactosidase activities are expressed in Miller Units (MU) (Miller, 1972) and results are

850 shown as the mean plus standard deviation of three biological replicates. A log scale is
851 applied for reasons of clarity.

852

853 **Figure 3. Functional studies of chimeric promoters derived from P_{bceA} (“B”) and P_{psdA}**
854 **(“P”).** Schematic of series of chimeric promoters (A) BP1-4, *bceA* promoter fragments (black)
855 with gradual substitutions of 3' region by increased corresponding parts of *psdA* promoter
856 (grey) and (B) PB1-4 vice versa are compared with WT P_{bceA} and P_{psdA} . The MBS and SBS of
857 P_{bceA} and P_{psdA} are represented as in Fig.1. Grey dashed lines indicate the fusion points of each
858 chimera. (C to H) Activities of chimeric promoters compared with WT promoters in different
859 genetic backgrounds of *B. subtilis*. Transcriptional *lacZ* fusions of WT promoters (P_{bceA} and
860 P_{psdA}) as well as different sets of chimeras (BP1-4 and PB1-4) were integrated at the *amyE*
861 locus of *B. subtilis* wildtype (WT), $\Delta psdRS$ strain (TMB1462) and $\Delta bceRS$ strain (TMB1460).
862 Promoter activities were measured by β -galactosidase assay as described in Fig. 2. (C) BP1-4
863 in WT, (D) BP1-4 in $\Delta psdRS$ strain, (E) BP1-4 $\Delta bceRS$ strain, (F) PB1-4 in WT, (G) PB1-4 in
864 $\Delta bceRS$ strain and (H) PB1-4 in $\Delta psdRS$ strain. For reasons of clarity, the values of promoter
865 activities induced by bacitracin are represented as % relative to the native P_{bceA} , while the
866 values of promoter activities induced by nisin are represented as % relative to the native P_{psdA}
867 promoters. Both wild type promoters are set to 100% after subtraction of the uninduced
868 promoter activities. The original data sets corresponding to Fig. 3 are provided in Fig. S1.
869 Black and grey bars, induction with bacitracin and nisin, respectively.

870

871 **Figure 4. Unravelling the roles of different promoter elements in RR-promoter**
872 **specificity.** (A and B) Schematic of chimeric promoters derived from P_{bceA} and P_{psdA} ,
873 respectively. Composition of each chimeric promoter is indicated as follows: M, main binding
874 site; L, linker; S, secondary binding site. MBS and SBS from P_{bceA} and P_{psdA} are indicated as
875 in Fig.1. (C to H) Activities of chimeric promoters compared with WT promoters in different

876 genetic backgrounds of *B. subtilis*. Transcriptional *lacZ* fusions of WT promoters (P_{bceA} and
 877 P_{psdA}) as well as different sets of chimeras from (A) and (B) were integrated at *amyE* locus in
 878 *B. subtilis* WT strain, $\Delta psdRS$ strain (TMB1462) and $\Delta bceRS$ strain (TMB1460). Promoter
 879 activities were measured by β -galactosidase assay as described for Fig. 2. (C) P_{bceA} -derived
 880 chimeras in WT, (D) P_{bceA} -derived chimeras in $\Delta psdRS$ strain, (E) P_{bceA} -derived chimeras in
 881 $\Delta bceRS$ strain, (F) P_{psdA} -derived chimeras in WT, (G) P_{psdA} -derived chimeras in $\Delta bceRS$ strain
 882 and (H) P_{psdA} -derived chimeras in $\Delta psdRS$ strain. Black bars and grey bars represent samples
 883 induced with bacitracin and nisin, respectively. Data representation as described for Fig. 3;
 884 original data sets are provided in Fig. S2.

885

886 **Figure 5. *In vitro* binding of BceR-P to P_{bceA} and P_{psdA} .** Increasing concentrations of
 887 phosphorylated 10 \times His-BceR were incubated with 30 fmol of different 6FAM-labeled
 888 promoter DNA fragments as follows: (A) P_{bceA} from -122 to +82, (B) P_{psdA} from -126 to +30,
 889 (C) P_{bceA} SBS^R (SBS inactivated), (D) P_{bceA} MBS^R (MBS inactivated), and (E) P_{sigW} as a
 890 negative control. Schematics of *bceA*-like promoters and corresponding mutants are shown in
 891 the lower left corner of each gel. The concentrations of phosphorylated BceR are indicated
 892 above the gel by [BceR-P] in μ M. 900 fmol of unlabelled competitor (comp.) DNA fragments
 893 containing P_{bceA} , P_{psdA} and P_{sigW} were added for lanes 6, 7 and 8, respectively, in (A) and (B).

894

895 **Figure 6. Surface plasmon resonance spectroscopy of and IM analysis BceR-P binding**
 896 **within the P_{bceA} and P_{psdA} promoter region.** (A) BceR binding to P_{bceA} , (B) BceR-P binding
 897 to P_{bceA} , (C) BceR-P binding to P_{bceA} MBS^R (MBS inactivated), and (D) BceR-P binding to
 898 P_{bceA} SBS^R (SBS inactivated), (E) IM and *in silico* sensorgrams of BceR binding to P_{bceA} ; (F)
 899 IM and *in silico* sensorgrams of BceR binding to P_{bceA} SBS^R (SBS inactivated), (G) BceR
 900 binding to P_{psdA} , (H) BceR-P binding to P_{psdA} , (I) BceR-P binding to P_{psdA} MBS^R, (K) BceR-P
 901 binding to P_{psdA} SBS^R, (L) IM and *in silico* sensorgrams of BceR binding to P_{psdA} , and (M)

902 IM and *in silico* sensorgrams of BceR binding to P_{psdA} SBS^R (SBS inactivated). SPR
903 sensorgrams: 0.2 nM (red line), 0.5 nM (brown line), 1 nM (dark blue line), 2.5 nM (magenta
904 line), 5 nM (green line), 7.5 nM (lime green line), and 10 nM (blue line), respectively, of each
905 of purified BceR or BceR-P was passed over the chip. The sensorgrams show each one
906 representative example of three independently performed experiments. IM analyses: the blue
907 spots in the IMs represent the fast ON/fast OFF interaction, which corresponds to the SBS, the
908 green spots the slow ON/slow OFF interaction corresponding to the higher affine MBS. The
909 respective calculated sensorgrams are shown in the same colors. The calculated overall
910 affinities (K_D), as well as the ON (k_a) and OFF (k_d) rates, are indicated below the respective *in*
911 *silico* sensorgram. The grey shapes of the IM peaks represent the weighing factors meaning
912 the darker the grey scale, the stronger the contribution.

913

914 **Figure 7. Model of the specific transcriptional activation of P_{bceA} by BceR and RNA**
915 **polymerase.** Initially, a BceR dimer (black), but not a PsdR dimer (grey) preferentially binds
916 to the MBS of P_{bceA} . This interaction then facilitates the binding of a second BceR dimer to
917 the SBS directly upstream of the -10 element of P_{bceA} . This second binding event then
918 mediates the binding of the σ^A subunit of the RNA polymerase holo-enzyme to the promoter
919 region to ultimately initiate transcription. Presumably, the structure of the DNA is altered by
920 the linker region between two binding sites (DNA bending). See discussion for details.

921

922 **Figure S1. Functional studies of chimeric promoters derived from P_{bceA} (“B”) and P_{psdA}**
923 **(“P”).** Schematic of series of chimeric promoters (A) BP1-4, *bceA* promoter fragments (black)
924 with gradual substitutions of 3' region by increased corresponding parts of *psdA* promoter
925 (grey) and (B) PB1-4 vice versa are compared with WT P_{bceA} and P_{psdA} . The MBS and SBS of
926 P_{bceA} and P_{psdA} are represented as in Fig.1. Grey dashed lines indicate the fusion points of each
927 chimera. (C to H) Activities of chimeric promoters compared with WT promoters in different

928 genetic backgrounds of *B. subtilis*. Transcriptional *lacZ* fusions of WT promoters (P_{bceA} and
929 P_{psdA}) as well as different sets of chimeras (BP1-4 and PB1-4) were integrated at the *amyE*
930 locus of *B. subtilis* wildtype (WT), $\Delta psdRS$ strain (TMB1462) and $\Delta bceRS$ strain (TMB1460).
931 Promoter activities were measured by β -galactosidase assay as described in Fig. 2. (C) BP1-4
932 in WT, (D) BP1-4 in $\Delta psdRS$ strain, (E) BP1-4 $\Delta bceRS$ strain, (F) PB1-4 in WT, (G) PB1-4 in
933 $\Delta bceRS$ strain and (H) PB1-4 in $\Delta psdRS$ strain. Black and grey bars, induction with bacitracin
934 and nisin, respectively; white bars, non-induced controls.

935

936 **Figure S2. Unravelling the roles of different promoter elements in RR-promoter**
937 **specificity.** (A and B) Schematic of chimeric promoters derived from P_{bceA} and P_{psdA} ,
938 respectively. Composition of each chimeric promoter is indicated as follows: M, main binding
939 site; L, linker; S, secondary binding site. MBS and SBS from P_{bceA} and P_{psdA} are indicated as
940 in Fig.1. (C to H) Activities of chimeric promoters compared with WT promoters in different
941 genetic backgrounds of *B. subtilis*. Transcriptional *lacZ* fusions of WT promoters (P_{bceA} and
942 P_{psdA}) as well as different sets of chimeras from (A) and (B) were integrated at *amyE* locus in
943 *B. subtilis* WT strain, $\Delta psdRS$ strain (TMB1462) and $\Delta bceRS$ strain (TMB1460). Promoter
944 activities were measured by β -galactosidase assay as described for Fig. 2. (C) P_{bceA} -derived
945 chimeras in WT, (D) P_{bceA} -derived chimeras in $\Delta psdRS$ strain, (E) P_{bceA} -derived chimeras in
946 $\Delta bceRS$ strain, (F) P_{psdA} -derived chimeras in WT, (G) P_{psdA} -derived chimeras in $\Delta bceRS$ strain
947 and (H) P_{psdA} -derived chimeras in $\Delta psdRS$ strain. Black bars and grey bars represent samples
948 induced with bacitracin and nisin, respectively, while white bars stand for non-induced
949 controls.

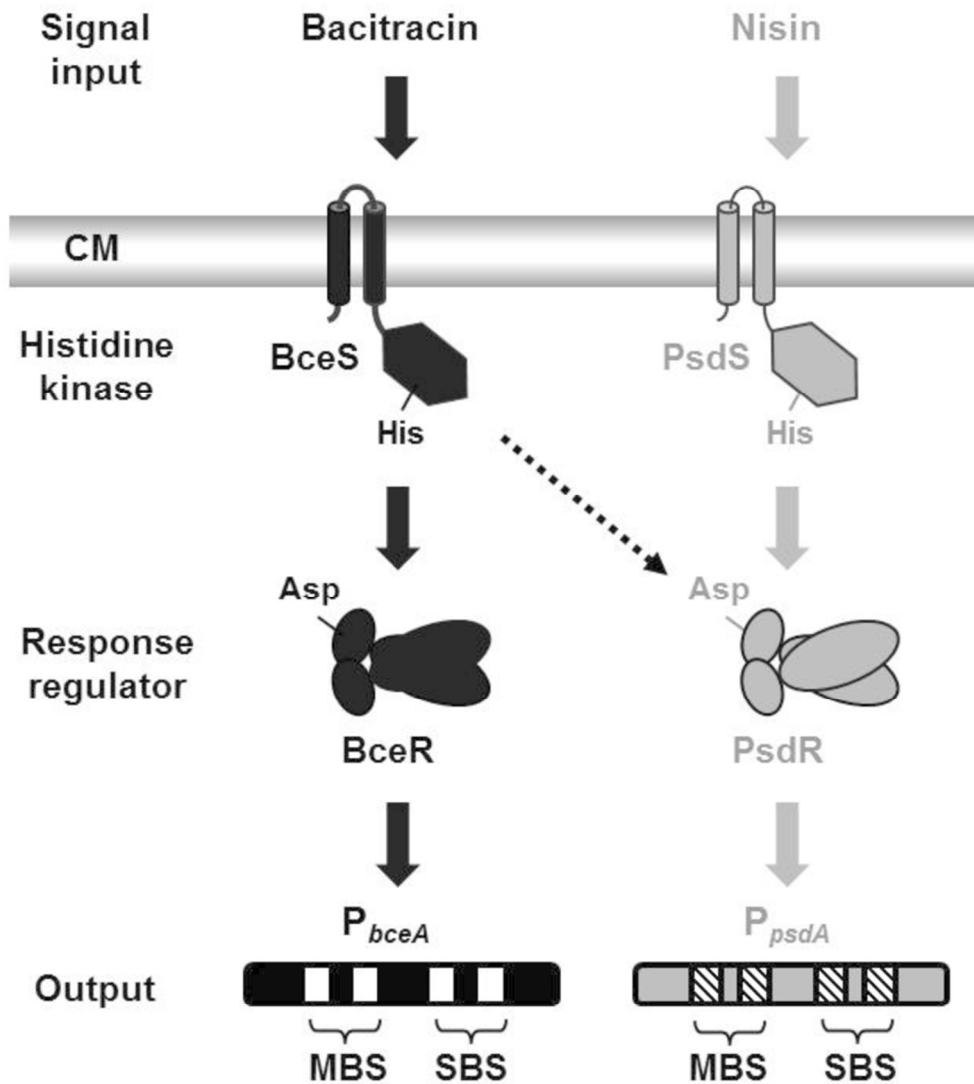


Figure 1. Model of signal transduction pathways of two Bce-like systems after induction with corresponding AMPs in *Bacillus subtilis*. The TCSs Bce and Psd and their inducing antibiotics as signal inputs are highlighted black and grey, respectively. For reasons of simplicity, the ABC transporters of both systems are not shown.

Solid arrows indicate the signal transduction pathway within one system, while cross-regulation between BceS and PsdR is highlighted by the dotted arrow. On each promoter, MBS representing for the main binding site and SBS representing for the secondary binding of Bce-like RRs are filled with white on *bceA* promoter and slashes on *psdA* promoter. CM, cell membrane.

85x94mm (300 x 300 DPI)

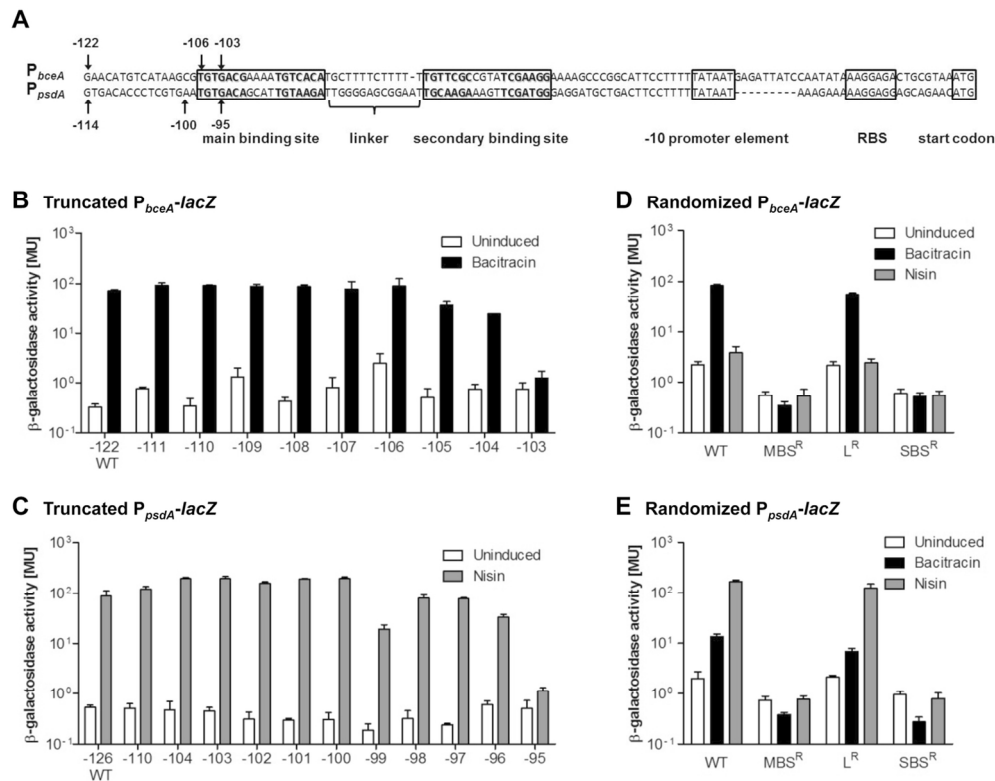


Figure 2. Functional analysis of *bceA* and *psdA* promoters of *B. subtilis*. (A) DNA sequence alignment of the *bceA* promoter and the *psdA* promoter. Different motifs are framed and annotated underneath the DNA sequence. Important positions on each promoter are marked with arrows according to the start codon of the corresponding regulated gene. Half binding sites of Bce-like RRs on each promoter are emphasized in bold face. Activities of (B) truncated constructions of the *bceA* promoter (from -122: +82 to -103: +82) and (C) truncated constructions of the *psdA* promoter (from -126: +30 to -95: +30) according to the start codon of regulated genes. Activities of (D) *P_{bceA}* mutants and (E) *P_{psdA}* mutants with MBSR (main binding site random mutation), LR (linker random mutation) and SBSR (secondary binding site random mutation) are compared with the corresponding WT promoters. All promoter constructions were fused to *lacZ* and introduced into *amyE* locus of *B. subtilis* 168. Cultures growing exponentially in LB were challenged with Zn²⁺-bacitracin 30 $\mu\text{g ml}^{-1}$ (black bars) or nisin 2 $\mu\text{g ml}^{-1}$ (grey bars) for 30 min, comparing with the non-induced condition (white bars). β -galactosidase activities are expressed in Miller Units (MU) (Miller, 1972) and results are shown as the mean plus standard deviation of three biological replicates. A log scale is applied for reasons of clarity.

124x98mm (300 x 300 DPI)

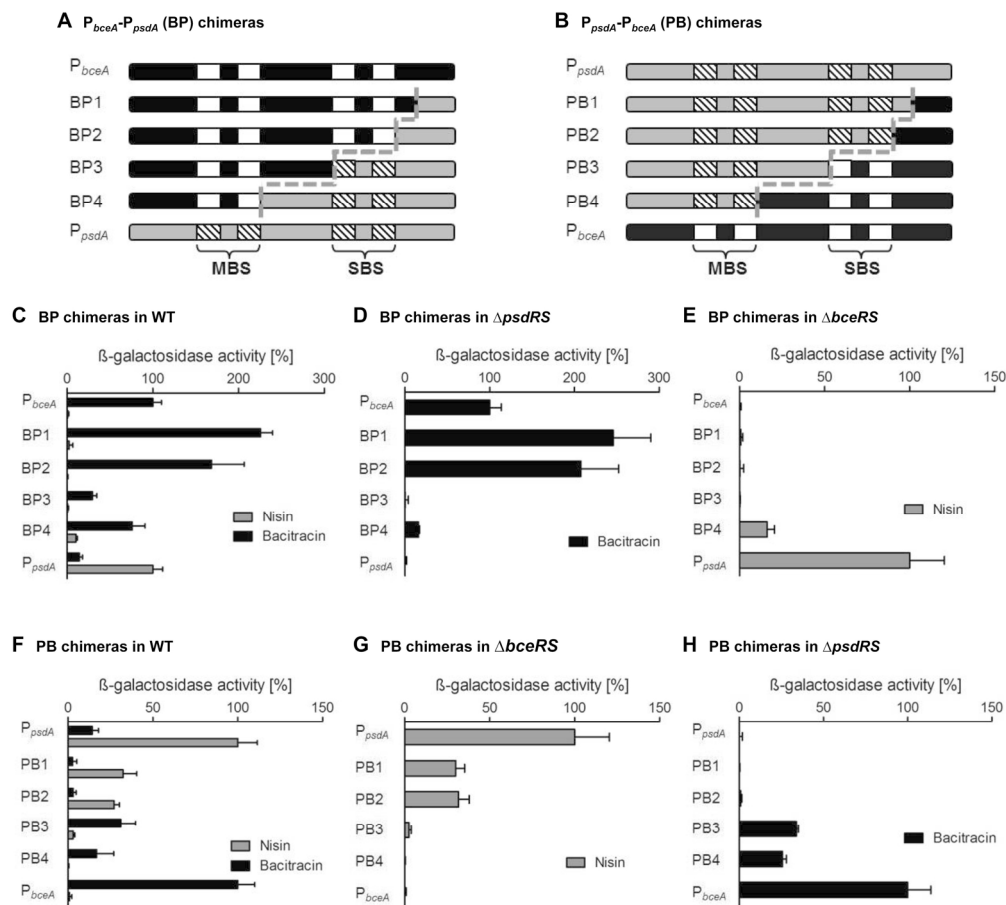


Figure 3. Functional studies of chimeric promoters derived from P_{bceA} ("B") and P_{psdA} ("P"). Schematic of series of chimeric promoters (A) BP1-4, $bceA$ promoter fragments (black) with gradual substitutions of 3' region by increased corresponding parts of $psdA$ promoter (grey) and (B) PB1-4 vice versa are compared with WT P_{bceA} and P_{psdA} . The MBS and SBS of P_{bceA} and P_{psdA} are represented as in Fig.1. Grey dashed lines indicate the fusion points of each chimera. (C to H) Activities of chimeric promoters compared with WT promoters in different genetic backgrounds of *B. subtilis*. Transcriptional *lacZ* fusions of WT promoters (P_{bceA} and P_{psdA}) as well as different sets of chimeras (BP1-4 and PB1-4) were integrated at the *amyE* locus of *B. subtilis* wildtype (WT), $\Delta psdRS$ strain (TMB1462) and $\Delta bceRS$ strain (TMB1460). Promoter activities were measured by β -galactosidase assay as described in Fig. 2. (C) BP1-4 in WT, (D) BP1-4 in $\Delta psdRS$ strain, (E) BP1-4 $\Delta bceRS$ strain, (F) PB1-4 in WT, (G) PB1-4 in $\Delta bceRS$ strain and (H) PB1-4 in $\Delta psdRS$ strain. For reasons of clarity, the values of promoter activities induced by bacitracin are represented as % relative to the native P_{bceA} , while the values of promoter activities induced by nisin are represented as % relative to the native P_{psdA} promoters. Both wild type promoters are set to 100% after subtraction of the uninduced promoter activities. The original data sets corresponding to Fig. 3 are provided in Fig. S1. Black and grey bars, induction with bacitracin and nisin, respectively.

173x161mm (300 x 300 DPI)

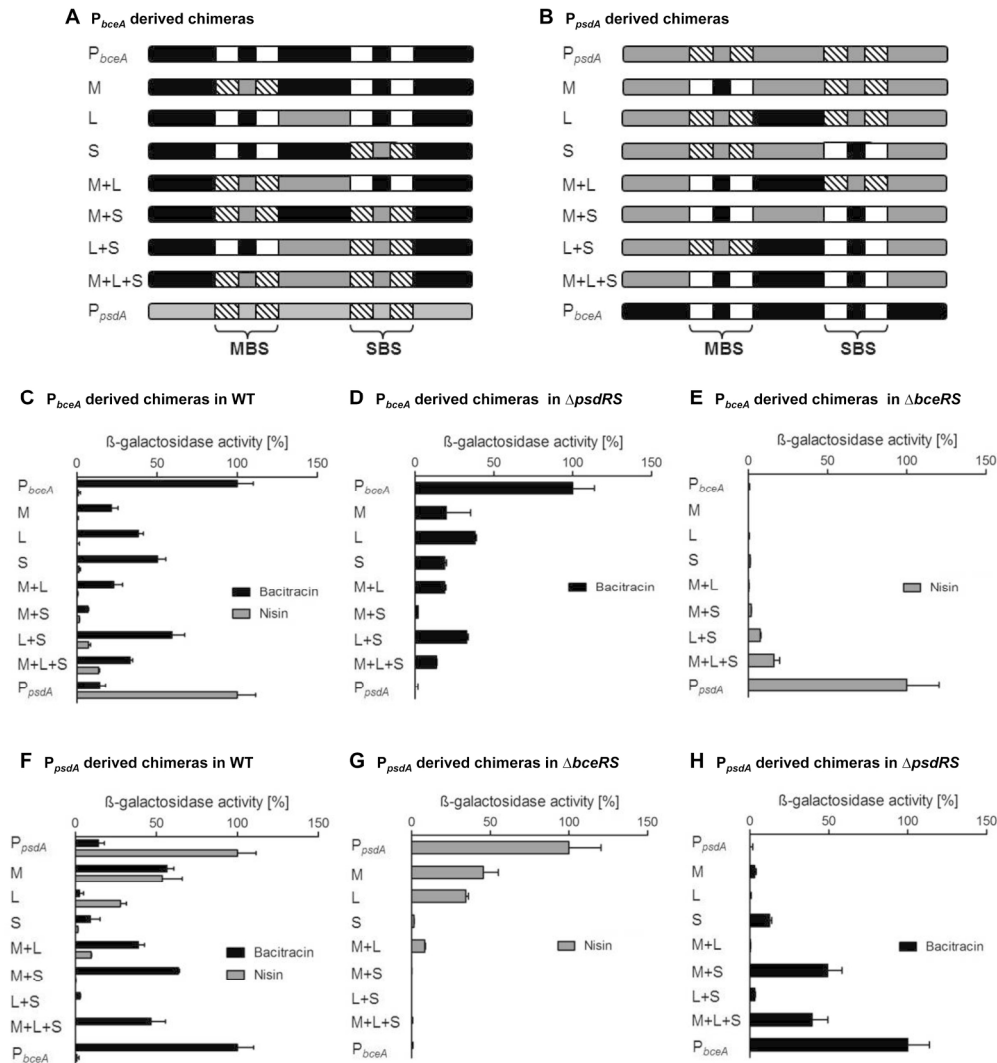


Figure 4. Unravelling the roles of different promoter elements in RR-promoter specificity. (A and B) Schematic of chimeric promoters derived from P_{bceA} and P_{psdA} , respectively. Composition of each chimeric promoter is indicated as follows: M, main binding site; L, linker; S, secondary binding site. MBS and SBS from P_{bceA} and P_{psdA} are indicated as in Fig.1. (C to H) Activities of chimeric promoters compared with WT promoters in different genetic backgrounds of *B. subtilis*. Transcriptional *lacZ* fusions of WT promoters (P_{bceA} and P_{psdA}) as well as different sets of chimeras from (A) and (B) were integrated at *amyE* locus in *B. subtilis* WT strain, $\Delta psdRS$ strain (TMB1462) and $\Delta bceRS$ strain (TMB1460). Promoter activities were measured by β -galactosidase assay as described for Fig. 2. (C) P_{bceA} -derived chimeras in WT, (D) P_{bceA} -derived chimeras in $\Delta psdRS$ strain, (E) P_{bceA} -derived chimeras in $\Delta bceRS$ strain, (F) P_{psdA} -derived chimeras in WT, (G) P_{psdA} -derived chimeras in $\Delta bceRS$ strain and (H) P_{psdA} -derived chimeras in $\Delta psdRS$ strain. Black bars and grey bars represent samples induced with bacitracin and nisin, respectively. Data representation as described for Fig. 3; original data sets are provided in Fig. S2.

200x215mm (300 x 300 DPI)

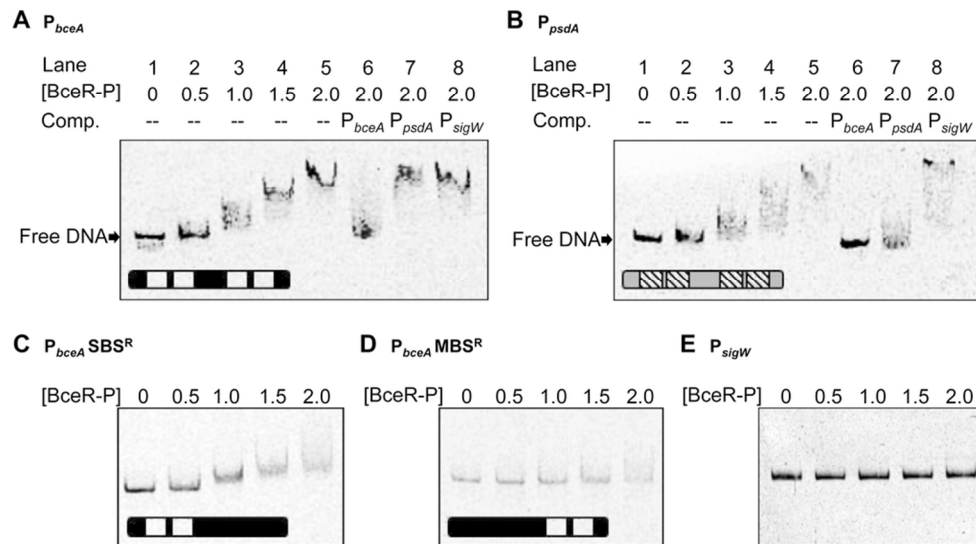


Figure 5. In vitro binding of BceR-P to P_{bceA} and P_{psdA} . Increasing concentrations of phosphorylated 10×His-BceR were incubated with 30 fmol of different 6FAM-labeled promoter DNA fragments as follows: (A) P_{bceA} from -122 to +82, (B) P_{psdA} from -126 to +30, (C) $P_{bceA}^{SBS^R}$ (SBS inactivated), (D) $P_{bceA}^{MBS^R}$ (MBS inactivated), and (E) P_{sigW} as a negative control. Schematics of $bceA$ -like promoters and corresponding mutants are shown in the lower left corner of each gel. The concentrations of phosphorylated BceR are indicated above the gel by [BceR-P] in μM . 900 fmol of unlabelled competitor (comp.) DNA fragments containing P_{bceA} , P_{psdA} and P_{sigW} were added for lanes 6, 7 and 8, respectively, in (A) and (B).

88x49mm (300 x 300 DPI)

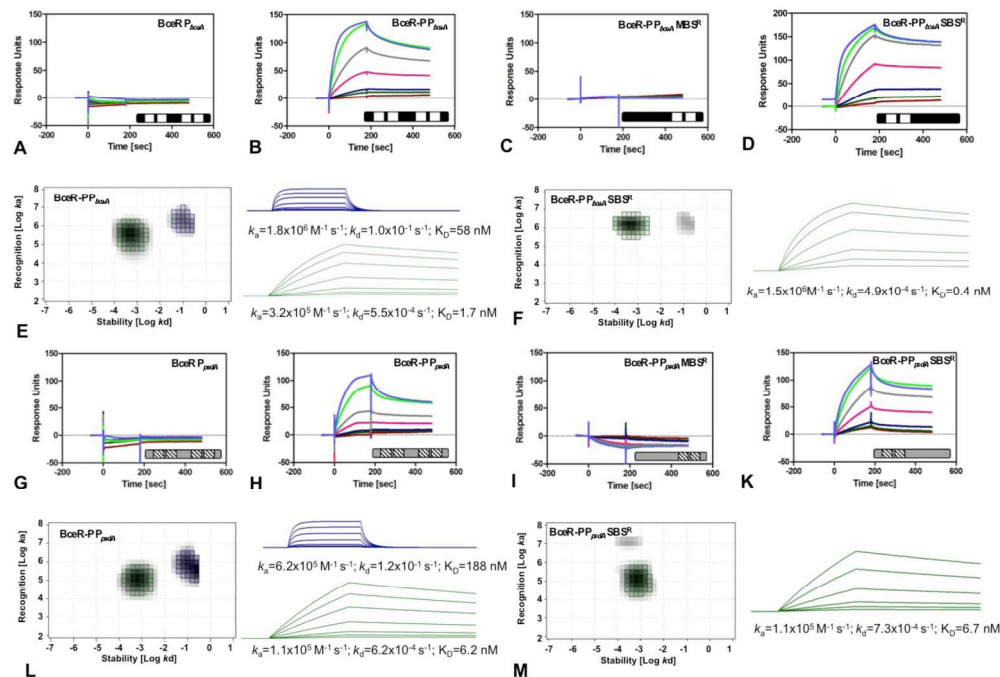


Figure 6. Surface plasmon resonance spectroscopy of and IM analysis BceR-P binding within the PbceA and PpsdA promoter region. (A) BceR binding to PbceA, (B) BceR-P binding to PbceA, (C) BceR-P binding to PbceA MBSR (MBS inactivated), and (D) BceR-P binding to PbceA SBSR (SBS inactivated), (E) IM and in silico sensorgrams of BceR binding to PbceA; (F) IM and in silico sensorgrams of BceR binding to PbceA SBSR (SBS inactivated), (G) BceR binding to PpsdA, (H) BceR-P binding to PpsdA, (I) BceR-P binding to PpsdA MBSR, (K) BceR-P binding to PpsdA SBSR, (L) IM and in silico sensorgrams of BceR binding to PpsdA, and (M) IM and in silico sensorgrams of BceR binding to PpsdA SBSR (SBS inactivated). SPR sensorgrams: 0.2 nM (red line), 0.5 nM (brown line), 1 nM (dark blue line), 2.5 nM (magenta line), 5 nM (green line), 7.5 nM (lime green line), and 10 nM (blue line), respectively, of each of purified BceR or BceR-P was passed over the chip. The sensorgrams show each one representative example of three independently performed experiments. IM analyses: the blue spots in the IMs represent the fast ON/fast OFF interaction, which corresponds to the SBS, the green spots the slow ON/slow OFF interaction corresponding to the higher affinity MBS. The respective calculated sensorgrams are shown in the same colors. The calculated overall affinities (KD), as well as the ON (k_a) and OFF (k_d) rates, are indicated below the respective in silico sensorgram. The grey shapes of the IM peaks represent the weighing factors meaning the darker the grey scale, the stronger the contribution.

170x117mm (300 x 300 DPI)

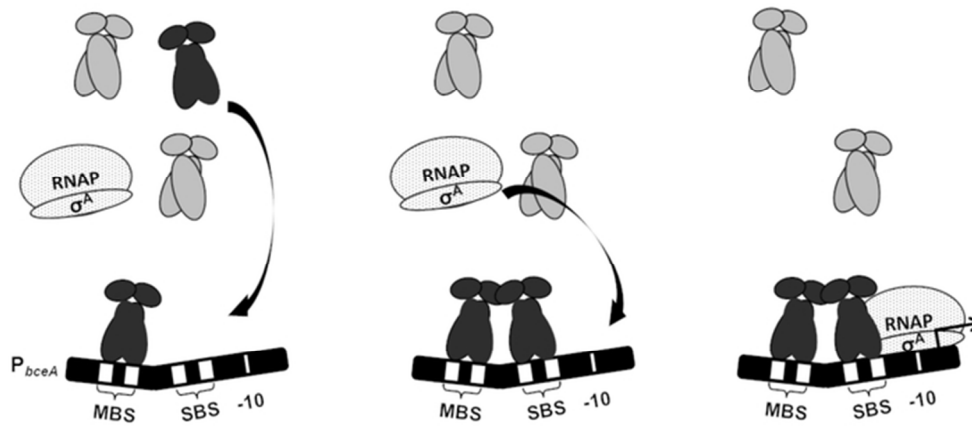


Figure 7. Model of the specific transcriptional activation of P_{bceA} by BceR and RNA polymerase. Initially, a BceR dimer (black), but not a PsdR dimer (grey) preferentially binds to the MBS of P_{bceA} . This interaction then facilitates the binding of a second BceR dimer to the SBS directly upstream of the -10 element of P_{bceA} . This second binding event then mediates the binding of the σ^A subunit of the RNA polymerase holoenzyme to the promoter region to ultimately initiate transcription. Presumably, the structure of the DNA is altered by the linker region between two binding sites (DNA bending). See discussion for details.

60x26mm (300 x 300 DPI)

Review